Cinnamoyl-CoA Reductase 1 (CCR1) and CCR2 Function Divergently in Tissue Lignification, Flux Control and Cross-talk with Glucosinolate Pathway in *Brassica napus*

Nengwen Yin,[1,2,†] Bo Li,[1,†] Xue Liu,[1] Ying Liang,[1,2] Jianping Lian,[1] Yufei Xue,[1] Cunmin Qu,[1,2] Kun Lu,[1,2] Lijuan Wei,[1,2] Rui Wang,[1,2] Jiana Li,[1,2,*] and Yourong Chai[1,2,*]

[1] Chongqing Engineering Research Center for Rapeseed, College of Agronomy and Biotechnology, Southwest University, Chongqing 400715, China

[2] Engineering Research Center of South Upland Agriculture of Ministry of Education, Academy of Agricultural Sciences, Southwest University, Chongqing 400715, China

[†]These authors contributed equally to this work.

[*] Address correspondence to ljn1950@swu.edu.cn and chaiyourong@163.com.

ORCID IDs: 0000-0002-9055-2030 (N.Y.); 0000-0002-9078-961X (B.L.); 0000-0002-3877-885X (X.L.); 0000-0001-9651-4564 (Y.L.); 0000-0003-2453-2266 (J.L.); 0000-0001-7041-5517(Y.X.); 0000-0003-2413-2350 (C.Q.); 0000-0003-1370-8633 (K.L.); 0000-0001-6405-0240 (L.W.); 0000-0002-7440-9197 (R.W.); 0000-0002-1605-8528 (J.L.); 0000-0001-6611-624X (Y.C.)

Running title: Divergent functions of *CCR1* and *CCR2* in *Brassica*

One sentence summary: *Brassica napus CCR1* and *CCR2* play divergent

roles in lignin monomers biosynthesis, tissue lignification, flux control, crosstalk with glucosinolate pathway and trait modifications when overexpressed.

Summary

Cinnamoyl-CoA reductase (CCR) is the entry point of lignin pathway and a crucial locus for traits dissection and manipulation. *Brassica* crops have worldwide importance, but their CCR-related metabolisms and traits are uncharacterized. Here, 16 *CCR* genes are identified from *B. napus* and its parental species *B. rapa* and *B. oleracea*. They are divided into *CCR1* subfamily and *CCR2* subfamily, which differ from each other in organ-specificity, participation in yellow-seed trait and responses to various stresses especially UV-B irradiation and *Sclerotinia sclerotiorum* infection. Their functions were dissected via overexpression of representative paralogs in *B. napus*. *BnCCR1* is preferentially involved in G- and H-lignin biosynthesis and vascular system development, while *BnCCR2* is preferentially involved in S-lignin biosynthesis and interfascicular fiber development. *BnCCR1* has stronger effects on lignification-related development, lodging resistance, flux control and seed color, whereas *BnCCR2* has stronger effect on sinapates biosynthesis. *BnCCR1* overexpressing plants show a delay in bolting and flowering, while *BnCCR2* overexpressing plants have less developed vascular system in leaf due to decreased G-lignin accumulation. Unexpectedly, both *BnCCR1* and *BnCCR2* overexpressors show no improvement in resistance to UV-B and *S. sclerotiorum*, implying complicated association of *Brassica CCR* with defense. Moreover, their glucosinolate profiles are greatly but almost oppositely remodeled through pathway crosstalk. Conclusively, *Brassica CCR1* and *CCR2* have great but divergent potentials in manipulating traits associated with phenylpropanoids and glucosinolates. This study provides systemic molecular and functional features of *B. napus CCR* family, and is the

first functional report on *CCR2* as well as *CCR1-CCR2* divergence in Brassicaceae.

Keywords: *Brassica*, Cinnamoyl-CoA reductase (CCR), Functional divergence, Lignin, Flavonoids, Glucosinolates, Lodging, *Sclerotinia sclerotiorum*.

Introduction

Lignins constitute one important group of phenylpropanoids, are deposited in plant secondary cell walls, and are the second most abundant biopolymers on the planet (Huang *et al*., 2010; Vanholme *et al.,* 2010). They perform many functions, providing structural support, giving rigidity and strength to stems to stand upright, and enabling xylems to withstand the negative pressure generated during water transport (Escamilla-Treviño *et al*., 2010; Labeeuw *et al*., 2015). In addition, lignins have been suggested to be induced upon various biotic and abiotic stresses, such as pathogen infection, insect feeding, drought, heat and wounding (Baucher *et al*., 1998; Caño-Delgado *et al*., 2003; Chantreau *et al*., 2014; Vanholme *et al*., 2010; Weng and Chapple, 2010).

To date, engineering of lignins mainly pursues reduced lignin content or altered lignin composition to meet the demands of agro-industrial processes, such as chemical pulping, forage digestibility, and the bioethanol production from lignocellulosic biomass (Baucher *et al*., 2003; De Meester *et al*., 2020; Ko *et al*., 2015; Li *et al*., 2008; Ragauskas *et al*., 2006; Weng *et al*., 2010). However, when altering the expression of lignin pathway genes, the metabolic flux of its neighbor pathways would be changed correspondingly (Besseau *et al*., 2007; Hoffmann *et al*., 2004; Li *et al*., 2010; Thévenin *et al*., 2011). Furthermore, dramatic modification of lignin content or lignin composition may provoke deleterious effects on plant growth, such as dwarfism and collapsed xylem vessels, with concomitant loss of biomass and yield (Berthet *et al*., 2011;

De Meester *et al*., 2020; Jones *et al*., 2001; Piquemal *et al*., 1998; Ruel *et al*., 2009).

Cinnamoyl-CoA reductase (CCR) is the entry point for the lignin-specific branch of the phenylpropanoid pathway and catalyzes the monolignol biosynthesis (Kawasaki *et al*., 2006; Lacombe *et al*., 1997). *Arabidopsis thaliana* possesses 11 annotated *CCR* homologs (Costa and Dolan, 2003), but only *AtCCR1* and *AtCCR2* encode true CCR enzyme (Lauvergeat *et al*., 2001). *AtCCR1* is preferentially expressed in tissues undergoing lignification, while *AtCCR2* is poorly expressed during development but is strongly and transiently induced by *Xanthomonas campestris*, suggesting that *AtCCR1* might be involved in constitutive lignification whereas *AtCCR2* might be involved in resistance (Lauvergeat *et al*., 2001). However, to date there is no functional verification of this assumption through over-expression transgenic study in *A. thaliana*, and the function of *CCR2* in Brassicaceae is not dissected. In monocot grasses, *CCR1* expression can be detected in various organs with a relatively high transcription level in stem (Giordano *et al*., 2014; Tu *et al*., 2010), thus is thought to be involved in constitutive lignification. In poplar and switchgrass, *CCR2* is expressed at very low levels in most organs, but can be significantly induced by biotic and abiotic stresses (Escamilla-Treviño *et al*., 2010; Fan *et al*., 2006). Manipulation of *CCR* (mainly through downregulation) typically results in a significant variation of lignin content and composition (Goujon *et al*., 2003; Wagner *et al*., 2013; Zhang *et al*., 2015; Zhou *et al*., 2010). Moreover, plants with dramatically downregulated *CCR* genes usually showed a stunted growth and delayed development (De Meester *et al*., 2020; Tamasloukht *et al*., 2011; Thévenin *et al*., 2011; van der Rest *et al*., 2006), and the alternation of carbon flux between lignin and other metabolic pathways was also accompanied (Dauwe *et al*., 2007; Tu *et al*., 2010; van der Rest *et al*., 2006; Wagner *et al*., 2013).

Lodging and diseases are fatal problems in field production of most crops.

Reducing plant height has been proven to be a useful strategy for improving lodging resistance, but dwarfism will reduce canopy photosynthetic capacity and yield (Acreche and Slafer, 2011; Peng *et al*., 2014; Tongyan *et al*., 2002; Zhang *et al*., 2001). Increasing stem strength would be a very promising strategy for breeding crops with high lodging resistance (Ma, 2009). Moreover, lignin is a physical barrier which can restrict pathogens to the infection site and confer disease resistance in plants (Lee *et al*., 2019). There are few reports at the molecular level to address how the regulation of lignin biosynthesis affects crop lodging and pathogen resistance via gene manipulation. In wheat, accumulation of lignin is closely related to lodging resistance, and wheat culms with higher lignin content could have a better lodging resistance (Peng *et al*., 2014). Regarding defense, the *CCR*-like gene *Snl6* is required for NH1-mediated resistance to bacterial pathogen *Xanthomonas oryzae* pv. *Oryzae* in rice (Bart *et al*., 2010). However, there is few reports on overexpressing *CCR* in enhancing lodging or disease resistance with molecular breeding values in crops.

Brassica, a relative genus of model plant *A. thaliana*, is of great importance since it contains various important oilseed, vegetable and ornamental crops. Unfortunately, *Brassica* crops especially rapeseed (*B. napus*) frequently suffer from some detrimental stresses such as lodging (Acreche and Slafer, 2011; Berry and Spink, 2012; Liu *et al*., 2010; Peng *et al*., 2014) and stem rot disease caused by *Sclerotinia sclerotiorum* with serious yield penalty and quality deterioration (del Río *et al*., 2007; Ding *et al*., 2015; Koch *et al*., 2007). In rapeseed, lodging could lead to 20%–46% yield loss and about four percent points of oil content reduction, and limits the efficiency of mechanical harvest (Berry, 2018; Kendall *et al*., 2017; Pan *et al*., 2012). There is little knowledge at present concerning the functional genes involved in lignin biosynthesis in rapeseed or even in *Brassica* species. Comprehensive characterization of the lignin biosynthesis in rapeseed will enable us to manipulate the lignin content or composition through genetic engineering, and to strengthen the capacity for lodging and pathogen resistance.

In this study, the *CCR1* and *CCR2* subfamily members from *B. napus* and its parental species *B. rapa* and *B. oleracea* were isolated, their expression patterns in different organs and under various stresses were investigated, and overexpression of *BnCCR1* and *BnCCR2* was performed for deciphering their biological functions and biotechnological potentials. Our results demonstrated that *BnCCR1* was mainly involved in the biosynthesis of H- and G-lignins, while *BnCCR2* showed a preference in the biosynthesis of S-lignin and in plant defense. A dramatic shift of carbon flux in phenylpropanoid pathway and a strong crosstalk effect on glucosinolate pathway was demonstrated in both *BnCCR1*- and *BnCCR2*-transgenic plants, especially for *BnCCR1* manipulation. Besides, *BnCCR1* and *BnCCR2* showed distinctly different association with flux regulation and development control, which accounted for distinct phenotypic modification in vascular system, lodging resistance, seed color, flowering time and glucosinolate profiles in corresponding overexpressors. Surprisingly and unexpectedly, both *BnCCR1*- and *BnCCR2*-overexpressors did not show increased resistance to *S. sclerotiorum* and UV-B light, implying complicated association of *CCR* and lignin pathway with disease resistance.

Results

Isolation and characterization of *CCR* genes from *Brassica* species

CCR genes were isolated from *B. napus* and its parental species *B. rapa* and *B. oleracea* using RACE strategy. Full-length cDNAs and corresponding gDNA sequences of three, four and six *CCR1*-subfamily gene sequences were isolated from *B. rapa*, *B. oleracea* and *B. napus*, while three, three and four *CCR2*-subfamily gene sequences were isolated from *B. rapa*, *B. oleracea*, respectively. Besides, one *CCR2* pseudogene from each parental species and two *CCR2* pseudogenes from *B. napus* were also isolated (Table S1). To determine the copy number of the *BnCCR1*, *BoCCR1*, *BrCCR1*, *BnCCR2*, *BoCCR2* and *BrCCR2* genes, Southern hybridization analysis was performed

(Figure S1), and the numbers of the clear bands were well correlated with the cloned gene sequence numbers. Table S1 shows all identity parameters of *CCR1*-subfamily and *CCR2*-subfamily genes/pseudogenes from *B. napus* and its parental species *B. oleracea* and *B. rapa* in terms of our cloning work and three genome datasets (NCBI GenBank, Genoscope and BRAD). The basic features of the cDNA and gDNA sequences are displayed in Table S2, and the deduced protein features are depicted in Table S3.

Multiple alignments showed that the conserved NADP binding domain and the CCR-featured traditional motif (KNWYCYGK, which was believed as the catalytic site) and novel motif $H_{202}K_{205}R_{253}$ (CCR-SBM or CCR substrate binding motif) are conserved in all *Brassica* CCRs (Chao *et al*., 2019; Lacombe *et al*., 1997). Therefore, it is speculated that these *Brassica* CCRs have catalytic activities. A phylogenetic tree was constructed to reveal the relationships of *Brassica* CCR1 and CCR2 proteins with CCRs from all whole-genome-sequenced species of other Brassicales species and other malvids orders (Figure S2). Firstly, it is clear that an early intrafamily duplication event generated the CCR1 and CCR2 groups within Brassicaceae, i.e. AtCCR1 and AtCCR2 have respective CCR1 and CCR2 orthologs only within Brassicaceae family. Secondly, in Brassicaceae the CCR1 group is much more conserved than the CCR2 group, which could be reflected by the great difference in branch lengths. Thirdly, outside the Brassicaceae family, other Brassicales families (e.g. Cleomaceae and Caricaceae) and other malvids orders (e.g. Malvales, Myrtales and Sapindales) have similar trends in CCR evolution (gene duplication and unequal divergence of paralogs) as revealed in Brassicaceae. However, paralog numbers (numbers of duplication events) vary distinctly among relative families and orders, and the single-copy CCR from Brassicales species *Carica papaya* is nearer to non-Brassicales CCRs than to other Brassicales CCRs.

Divergent involvement in organ-specificity and seed coat color among

***Brassica CCR* family members**

In all the three *Brassica* species the highest *CCR1* subfamily expression was detected in silique pericarp, while the highest *CCR2* subfamily expression varied among species (bud in *B. napus*, silique pericarp in *B. rapa*, and root in *B. oleracea*), implying faster divergence of organ-specificity in *CCR2* than in *CCR1* among species. Within each species, divergence of organ-specificity and expression intensity among *CCR* paralogs were distinct, and generally stronger divergence of organ-specificity among *CCR2* paralogs could be observed than among *CCR1* paralogs. For *CCR1* subfamily, *BnCCR1-2*, *BrCCR1-2* and *BoCCR1-1* were the dominant paralog within respective species. For *CCR2* subfamily, *BnCCR2-4*, *BrCCR2-1A* and *BoCCR2-2* were the dominant paralog within respective species (Figures S3-S6). In all the three species, *CCR1* subfamily overall expression was distinctly lower in developing seeds especially in late-stage seeds of yellow-seed stocks than in black-seed stocks, whereas *CCR2* subfamily showed an opposite trend (Figures S3-S6).

Differential responsiveness to various stresses between *BnCCR1* and *BnCCR2* subfamilies

For *BnCCR1*, its overall expression showed limited upregulations by NaCl, drought & high temperature and UV-B treatment, while kept almost constant when treated with other stresses (Figure S7). Under the same stresses, both the overall and the member-specific expressions of *BnCCR2* subfamily were dramatically upregulated. Its overall expression in leaves was upregulated by 400.3 folds at 48 h after *S. sclerotiorum* inoculation, by 49.59 folds at 80 min after UV-B treatment, by 10.75 folds at 48 h after *P. rapae* inoculation, and with slow and slight increase after high temperature & drought treatment (Figures S7 and S8). All *BnCCR2* subfamily members could be triggered by these stresses, and *BnCCR2-4* was dominant among paralogs (Figure S8). Although both *BnCCR1* and *BnCCR2* subfamilies can be distinctly regulated by multiple stresses, *BnCCR1* only mildly responds to abiotic stresses, while *BnCCR2* responds sharply and intensively to both biotic and abiotic stresses, thus *BnCCR2* is speculated to play more important roles than *BnCCR1* in coping

with various stresses in *B. napus*.

BnCCR* over-expression dramatically influenced plant morphology, but did not increase resistance to UV-B and *S. sclerotiorum

To further uncover the function of *Brassica CCR* genes, overexpression transgenic plants were generated. *BnCCR1-2* and *BnCCR2-4* were selected for transgenic study as they are dominant members within respective subfamilies. The transgenic lines were coded as *BnCCR1-2ox* or ox1 lines for *BnCCR1-2* overexpression, and *BnCCR2-4ox* or ox2 lines for *BnCCR2-4* overexpression, in the following analysis. The transgenic lines were screened along with non-transgenic controls (WT) by GUS staining, Basta resistance and PCR detection (Figure S9). Six *BnCCR1-2ox* and seven *BnCCR2-4ox* triple-positive lines were obtained, with different over-expression levels revealed by qRT-PCR detection (Figure S10).

All *BnCCRox* plants showed a stronger morphological development than WT throughout the whole life (Figure 2). Both *BnCCR1-2ox* and *BnCCR2-4ox* had larger and longer leaves, higher leaf chlorophyll content, larger stem diameter, wider silique, higher breaking-resistant stem strength, better lodging resistance and more siliques per plant, with distinctly stronger effects in *BnCCR1-2ox* lines than in *BnCCR2-4ox* lines (Figure 2; Figures S11 and S12). Phytohormone detection showed that abscisic acid (ABA) increased significantly in the leaves of *BnCCRox* lines compared with WT (Figure S13). The leaves of *BnCCR1-2ox* had more obvious wrinkles and less leaf margin serrates than WT (Figure 2c; Figure S12e). *BnCCR2-4ox* plants had a looser morphology with larger leaf angles (Figure 2b and j), and their leaves were more easily to show bending and rollover phenomenon than WT when under strong sunlight and high temperature conditions (Figure S12d). On the other hand, upper stems of *BnCCR1-2ox* plants at late bolting stage were more easily to appear bending phenomenon, but this phenomenon would disappear after flowering stage (Figure 2f-i; Figure S12a). Moreover, *BnCCR1-2ox* lines flowered 7-10 days later than WT on average, and this phenomenon varied among years and environments. However, *BnCCR2-4ox* plants had no significant difference in flowering time when compared with WT. Interesting

phenomenon was observed on petiole-vein system, which was distinctly larger in transgenic plants than WT, but phloroglucinol-HCl staining showed that petiole-vein lignification was strengthened only in *BnCCR1-2ox* plants while was weakened in *BnCCR2-4ox* plants (Figure 2d; Figure S12f, h and j). Seed yield per plant of *BnCCR1-2ox* had little difference compared with WT, but *BnCCR2-4ox* had slightly decreased seed yield (Figure S11l). Besides, both *BnCCR1-2ox* and *BnCCR2-4ox* plants exhibited no better resistance to *S. sclerotiorum* inoculation and UV-B treatment when compared with WT, even some transgenic lines had a little reduction in disease resistance in leaf identification (Figure S14a, b, e and h).

Yellow-seed traits generated in *BnCCRox* lines

As displayed in Figure 3a, the seed color of both *BnCCR1-2ox* and *BnCCR2-4ox* turned lighter compared with WT, and *BnCCR1-2ox* showed a stronger effect than *BnCCR2-4ox*. Microscopic investigation of the frozen sections of seed coat (Figure 3b) and R value obtained through NIRS assay (Figure 3e) further proved this effect. However, the thickness of the seed coat had no significant difference between *BnCCRox* and WT, which was different from traditionally bred yellow-seeded cultivars which usually had thinner seed coat than black-seeded cultivars (Qu *et al*., 2013; Zhang *et al*., 2013). As expected, the *BnCCR1-2ox* seed coat had an apparent reduction of condensed tannin compared with WT, e.g. ox1-5, ox1-8, ox1-12 and ox1-14 had a decrease of 69%, 29%, 40% and 57% respectively (Figure 3c and g). But unexpectedly, a significant increase was found for *BnCCR2-4ox* seed coat when compared with WT, e.g. ox2-4, ox2-11, ox2-16 and ox2-25 showed an increase of 88%, 300%, 158% and 83% respectively (Figure 3c and g), implying looser condensation of the tannin structure caused by unknown mechanisms. Furthermore, all *BnCCRox* lines had a significant reduction of the thousand-seed weight, with *BnCCR1-2ox* lines reduced by 10%-20%, and *BnCCR2-4ox* lines reduced by 15%-30% (Figure 3d). Surprisingly, the NIRS detection results showed that the total glucosinolates content of *BnCCR1-2ox* lines had a considerable increase compared with WT and a decline in *BnCCR2-4ox* lines (Figure 3f).

BnCCR over-expression greatly changed lignification phenotypes

The frozen cross sections of stem middle part at early flowering stage and stem middle-lower part at maturing stage were investigated (Figure 4a-c), which displayed that both *BnCCR1-2ox* and *BnCCR2-4ox* stems had an changed shape with more concave and convex and a wider xylem parts with deeper histochemical staining, and some extreme *BnCCR1-2ox* lines appeared an ectopic lignin deposition as shown in Figure 4c. Observed with higher amplification folds of the sections, *BnCCR1-2ox* showed a better developed xylem part, had more number and more concentrated vessels with deeper brown color (indicating more G-lignin unit) in Mäule staining in which G- and S-type lignin units could be stained brown and red respectively (Figure 4f and g, early flowering stage), with brighter red phloroglucinol-HCl staining (Figure 4h, mature stage) and brighter blue fluorescence (Figure 4i and j, early flowering stage) as compared with WT. These indicated that *BnCCR1-2ox* stems contained higher level of lignin content compared with WT. *BnCCR2-4ox* stem sections also displayed a better developed xylem part and interfascicular fiber part. Although its vessel number and size were not obviously different from WT, there was a significant deeper red color (indicating S-lignin unit) in both Mäule staining (Figure 4f and g) and phloroglucinol-HCl staining (Figure 4h), especially to the interfascicular fiber cells wall, and brighter blue florescence under UV light (Figure 4i and j) compared with WT. This result indicated that *BnCCR2-4ox* stems had higher proportion of S-lignin besides with higher total lignin content. Similar enhancement trends of the lignification pattern were also found in detection results of siliques (Figure 4k-n).

This study also reveals that rapeseed has two types of roots: type I with higher proportion of interfascicular fibers, while type II with higher proportion of vessels (Figure 4d and e). In *BnCCR1-2ox* and *BnCCR2-4ox* lines, both type I and type II roots displayed a better developed xylem tissues with bigger size and more concentrated vessels, and had a deeper staining by

phloroglucinol-HCl method compared with WT (Figure 4d and e). Besides, type II roots of *BnCCR1-2ox* showed a significantly better vessel development (Figure 4e) than WT and *BnCCR2-4ox*. Through comparison of the above-mentioned histochemical staining assay or fluorescence excitation assay of stems and roots, *BnCCR1-2ox* had better developed vascular bundles, while *BnCCR2-4ox* had better developed interfascicular fibers than WT (Figure 4d, g, h and j).

For leaf traits, the petiole of *BnCCR1-2ox* tended to be more circular with more and better developed vascular bundles (Figure 4o and q). But for *BnCCR2-4ox* lines, it was smaller than WT and developed asymmetrically with fewer and less developed vascular bundles (Figure 4o and q), maybe this was one reason that caused *BnCCR2-4ox* leaves much easier to bend and rollover than WT when under strong sunlight and high temperature conditions. Moreover, *BnCCR1-2ox* lines had a deeper brown color in Mäule staining and had a brighter blue fluorescence under UV light than WT (Figure 4p and q), which indicated that *BnCCR1-2ox* petiole xylem contained higher lignin content as well as higher G-lignin proportion. The *BnCCR2-4ox* petiole sections displayed no better Mäule staining, and the blue fluorescence was significant weaker than WT (Figure 4q), which indicated that *BnCCR2-4ox* petiole xylem contained less lignin content which was consistent with phloroglucinol-HCl staining of leaves (Figure S12j).

Notable changes in content and structure of lignins in *BnCCR* over-expression lines

Biochemical analysis showed that the acetyl-bromide soluble lignin content of both *BnCCR1-2ox* and *BnCCR2-4ox* was significantly increased compared to WT (Figure 4r-t). The lignin content of stems of *BnCCR1-2ox* lines ox1-5, ox1-8, ox1-12 and ox1-14 increased by 24%, 34%, 23% and 15%, respectively (Figure 4r). For *BnCCR2-4ox* lines ox2-4, ox2-11, ox2-16 and ox2-25, their stem lignin content increased by 40%, 25%, 31% and 51%, respectively (Figure 4r). In roots, the lignin content of ox1-5, ox1-8, ox1-12, ox1-14, ox2-4,

ox2-11, ox2-16 and ox2-25 increased by 0.4%, 18%, 15%, 5%, 18%, 25%, 12% and 23% compared with WT, respectively (Figure 4s). Similar trends also happened in seed coat of *BnCCR1-2ox* lines (Figure 4t). Similar to tannin detection result, the seed coat lignin content of the *BnCCR2-4ox* lines increased by 92%-130% (Figure 4t), implying possible decreased lignin polymerization.

S/G ratio, which was typically used to characterize the lignin structure, changed significantly in both stems and roots of *BnCCRox* lines. In the stems of both *BnCCR2-4ox* and WT, their lignin had higher content of S-unit than G-unit, and the S/G ratio was increased by 20.2% and 22.5% in ox2-4 and ox2-16 compared with WT (Figure 4w). It was mainly attributed to their greater proportion of S-lignin content (Figure 4u and w; Figure S15), which was in consistent with the Mäule staining results. However, in the case of the stems of *BnCCR1-2ox* lines, the G-unit, other than S-unit, served as the main lignin units, so it was contrary to *BnCCR2-4ox* and WT. Due to increased G-unit proportion, the S/G ratio in the stems of ox1-5 and ox1-12 decreased by 47.3% and 24.0%, respectively, compared to WT (Figure 4u and w; Figure S15). In roots, the alteration tendency of S/G ratio of ox1-5 and ox2-16 was similar to that in stems, decreased to 0.22 and increased to 0.78, respectively as compared with WT (0.49) (Figure 4x).

Another striking change was H-lignin proportion, which generally had trace amount in dicotyledonous stems (usually no more than 1%). The H-lignin content of ox1-5 and ox1-12 was about four and three folds of the WT respectively, while was increased by only about 50% in ox2-4 and ox2-16 (Figure 4u; Figure S15). In the root of ox1-5, the H-lignin content also had an obvious increase, reaching about two folds of WT amount (7.43% of WT VS 15.59% of ox1-5) (Figure 4v; Figure S15). In conclusion, the lignin structure of *B. rapus* was undoubtedly modified after the manipulation of *BnCCR* genes. However, the NIRS results indicated that cellulose and hemicellulose contents of both *BnCCR1-2ox* and *BnCCR2-4ox* lines had no significant difference when compared with WT (Figure S16).

Metabolic remodeling of phenylpropanoid and glucosinolate pathways

by over-expressing *BnCCR1* and *BnCCR2*

The drastic alteration of seed color, seed coat condensed tannin content, lignin content, lignin structure and plant phenotypes all indicated flux change within and outside the lignin biosynthetic network in *BnCCR* overexpressors.

Conforming to prediction, most phenolic compounds synthesized at the downstream of CCR were apparently increased in the stems of ox1-5 and ox2-16 lines, including sinapoylhexose, sinapic acid, sinapoyl malate, ferulic acid, feruloyl malate, *p*-coumaraldehyde and 1,2-disinapoylglucoside, with an increase of about 1-10 folds, and ox2-16 displayed stronger effects than ox1-5 (Figure 5a; Table S4). However, flavonoids in ox1-5 stems were reduced to 3%-71% of WT, including km-3-O-sophoroside-7-O-glucoside, rutin, is-3-sophoroside-7-glucoside, km-3-O-sinapoylsophoroside-7-O-glucoside, qn-3-O-sophoroside, qn-3-O-glucoside, km-3-O-glucoside and is-3-O-glucoside; and ox2-16 showed the same trend as ox1-5 but with a less extent (Table S4). Leaf extracts of ox1-5 and ox2-16 had similar variation tendency as in stems, but some compounds were undetectable in leaves or had an opposite change (Table S4). Metabolites profiling was also performed on 30 DAP seeds. As expected, the CCR-downstream compounds sinapic acid and disinapoylgentiobiose were significantly increased in ox1-5 and ox2-16 (Table S5). The contents of the most compounds of epicatechin, procyanidin, epicatechin polymers and other important flavonoids were significantly reduced (by even more than 90% for some flavonoids) in ox1-5 compared with wild type, and ox2-16 showed the same trend as ox1-5 but with a less extent (Figure 5b; Table S5). However, the kaempferol derivatives km-3-O-diglucoside and km-3-O-sophoroside were exceptionally increased in transgenic seeds.

In metabolic profiling, glucosinolates were unexpectedly found to be drastically changed by *BnCCR* overexpression. A variety of aliphatic glucosinolates were distinctly differentially deposited between *BnCCRox* lines

and WT. For example, 2(R)-2-hydroxy-3-butenyl glucosinolate, 1-S-[(3S)-3-Hydroxy-N-(sulfooxy)-5-hexenimidoyl]-1-thio-beta-D-glucopyranose, 3-butenylglucosinolate, isobutyl glucosinolate, 4-pentenyl glucosinolate, 5-methylsulfinylpentyl glucosinolate and 5-methylthiopentyl glucosinolate were upregulated to hundreds of folds or even more than 1000 folds in ox1-5 stems as compared with WT, while in ox2-16 stems they were just slightly upregulated or even downregulated (Figure 5c; Table S4). In addition, 1-S-[(3S)-3-Hydroxy-N-(sulfooxy)-5-hexenimidoyl]-1-thio-beta-D-glucopyranose was obviously accumulated in both types of transgenic plants, and 4-methylthiobutyl glucosinolate and 6-methylthiohexyl glucosinolate were obviously accumulated in ox1-5 stems (not in ox2-16 and WT stems). According to the quantitative results, glucosinolates had larger amounts of accumulation in leaves than in stems (Table S4), and most of them in leaves were several folds higher in ox1-5 than in WT. However, most of them were downregulated by hundreds of folds in the leaves of ox2-16 in comparison with WT. 2(R)-2-Hydroxy-3-butenyl glucosinolate, 1-S-[(3S)-3-Hydroxy-N-(sulfooxy)-5-hexenimidoyl]-1-thio-beta-D-glucopyranose and 5-methylthiopentyl glucosinolate were even not detectable in the leaves of ox2-16 (Table S4). Glucosinolates variation in seed coat was similar to that in the leaf (Tables S5). Modification of secondary metabolites in petioles was ultimately similar to that in stems (Tables S6).

Differential redirection of gene expression in lignin, flavonoid and glucosinolate pathways in *BnCCR1* and *BnCCR2* over-expressors

In *BnCCR1-2ox* lines, *BnCCR1* subfamily itself was significantly upregulated, and *BnCCR2* subfamily showed no significant upregulation. In *BnCCR2-4ox* lines, the *BnCCR2* subfamily itself was undoubtedly greatly upregulated, while *BnCCR1* subfamily was also significantly upregulated (1-3 folds) in the stems, petioles and 30DAP seeds but significantly downregulated by 70% in the leaves (Figure S17). These results indicated that over-expression of *BnCCR1*

subfamily had little impact on the expression of *BnCCR2* subfamily, but over-expression of *BnCCR2* subfamily could significantly upregulate or downregulate the expression of *BnCCR1* subfamily depending on different organs.

In the stems of both *BnCCR1-2ox* and *BnCCR2-4ox* lines, the common phenylpropanoid pathway loci *C4H* and *4CL* and the lignin-pathway early-step loci *C3H*, *HCT* and *CCoAOMT* were mildly upregulated (Figure 6a), and *CCR*-downstream loci *CAD* and *F5H* were slightly upregulated. *COMT* was specific, apparently upregulated in the stems of *BnCCR1-2ox*, but downregulated to less than 10% in the stems of *BnCCR2-4ox* as compared with WT.

On the other hand, the expression of the flavonoid biosynthesis pathway was significantly downregulated in *BnCCRox* lines. Regulatory genes *TT1*, *TT2*, *TT16*, *TTG1* and *TTG2*, and structural genes *CHS*, *CHI*, *F3H*, *F3'H*, *FLS*, *ANR*, *TT19*, *GSTF11* and *TT12* were all suppressed to certain extent in 30DAP seeds of both *BnCCR1-2ox* and *BnCCR2-4ox* (Figure 6b), with less extent in *BnCCR2-4ox* than in *BnCCR1-2ox*. *CHS*, *CHI*, *F3H*, *ANR* and *TT19* were downregulated to less than 20% in the 30DAP seeds of ox1-5 when compared with WT (Figure 6b). The structural genes *AHA10* and *TT10* and the regulatory genes *TT8* and *MYB111* were significantly downregulated in 30DAP seeds of *BnCCR2-4ox*, but were unexpectedly significantly upregulated in the 30DAP seeds of *BnCCR1-2ox* lines (Figure 6b). The overall downregulation of the whole flavonoid pathway could account for the reduction of the flavonoids in *BnCCRox* lines.

Most of the genes associated with the aliphatic glucosinolate biosynthesis, such as *MYB28*, *MYB29*, *CYP79F1*, *CYP83A1*, *AOP2* and *GSL*, were significantly upregulated in *BnCCR1ox* lines (Figure 6c). Especially, the expression of *MYB29*, *CYP79F1* and *GSL* could hardly be detected in WT and *BnCCR2ox* lines, but was considerably expressed in *BnCCR1ox* lines. *AOP2*

was a specific locus, which showed considerable downregulation in *BnCCR2ox*, a trend opposite to that in *BnCCR1ox* (Figure 6c). The expression of most genes involved in indole glucosinolate biosynthesis, such as *MYB122*, *CYP79B2*, *ST5a* and *IGMT1*, was dramatically decreased in both *BnCCR1ox* and *BnCCR2ox* lines, except that *MYB34* was significantly upregulated in both *BnCCR1ox* and *BnCCR2ox* lines (Figure 6c). *MYB51* was significantly upregulated in *BnCCR1ox* lines but extremely downregulated in *BnCCR2ox* lines, implying that *MYB51* may also be involved in aliphatic glucosinolate biosynthesis in *B. napus*.

Discussion

Both *BnCCR1* and *BnCCR2* are crucial for lignification, associated with different monolignols and cellular types

Plants with downregulated CCR activities often displayed reduction in lignin content and alteration in lignin structure depending on different species (Goujon et al., 2003; Leplé et al., 2007; Prashant et al., 2011; van der Rest et al., 2006; Zhou et al., 2010). Lignin content had a great decrease in *Arabidopsis CCR1* mutant *irx4* (Jones *et al*., 2001) and *CCR*-suppressed transgenic *Arabidopsis* (Goujon *et al*., 2003), tobacco (Piquemal *et al*., 1998), poplar (Leplé *et al*., 2007), *Medicago truncatula* (Zhou *et al*., 2010) and perennial ryegrass (Tu *et al*., 2010).

In this study, anatomical observation and histochemical staining both indicated significant improvement of lignification in stems and roots in both *BnCCR1* and *BnCCR2* over-expressors, and *BnCCR1* over-expressor showed stronger effect on development of vessels and vascular bundles in xylem, while *BnCCR2* over-expressor showed stronger effect on interfascicular fibers. In biochemical detection, lignin content was significantly increased in both *BnCCR1-2ox* and *BnCCR2-4ox*, suggesting that both *BnCCR1* and *BnCCR2* subfamilies play a pivotal role in lignin biosynthesis in *B. napus*.

Furthermore, the S/G ratio was significantly decreased in *BnCCR1-2ox*, mainly due to the stronger increase of G-lignin which was in accordance with the Mäule staining results. In contrast, the S/G ratio in *BnCCR2-4ox* was significantly increased, mainly attributed to stronger increase of S-lignin. The alteration of S/G ratio caused by *CCR* manipulation always had different trends in different species. A lower S/G ratio, mainly caused by relatively stronger effect of *CCR* downregulation on S-units, was observed on *Arabidopsis irx4* mutants (Patten *et al*., 2005), *CCR*-downregulated poplar (Leplé *et al*., 2007) and *ccr1*-knockout *M. truncatula* mutants (Zhou *et al*., 2010). A higher S/G ratio, mainly caused by relatively stronger effect of *CCR* downregulation on G-units, was found in *CCR*-downregulated tobacco (Chabannes et al., 2001; Piquemal et al., 1998), maize (Tamasloukht *et al*., 2011), dallisgrass (Giordano *et al*., 2014) and *CCR2*-knockout *M. truncatula* mutants (Zhou *et al*., 2010). No obvious change of S/G ratio was recorded in poplar (Leplé *et al*., 2007) and perennial ryegrass with *CCR* manipulation (Tu *et al*., 2010).

The H-lignin percentage in the stems of *BnCCR1-2ox* was 2-3 folds higher than WT, and also more than one fold higher in roots. Which could be caused by the enhanced accumulation of *p*-coumaraldehyde and expression of *F5H* and *COMT* in *BnCCR1-2* over-expressor. Reasonably, *p*-coumaroyl-CoA and caffeoyl-CoA might serve as the primary substrates for BnCCR1 (as suggested in Figure 7). The caffeoyl aldehyde could be derived from the *p*-coumaraldehyde, and could also form coniferaldehyde through F5H and COMT catalysis (these two enzymes could mediate the hydroxylation and methylation of the C3 on the aromatic ring, Figure 7). In *CCR1*-downregulated perennial ryegrass (Tu *et al*., 2010) and Mu-insertion maize mutant *Zmccr1*$^{-}$ (Tamasloukht *et al*., 2011), the H-subunit level was reduced by about 50% and 31% respectively, suggesting that the optimal substrate of CCR1 of perennial ryegrass and maize was *p*-coumaroyl-CoA. On the other hand, BnCCR2 might prefer feruloyl-CoA as its major substrate, because of higher accumulation of S-units and its downstream derivatives sinapate esters, and higher increase in transcript level of *F5H* in *BnCCR2ox* as compared with *BnCCR1ox* (Figure 7).

Upregulation of *BnCCR* genes enhanced lodging resistance, modified morphology, but did not improve disease and UV-B resistance

The expression perturbation of the genes located at the lignin biosynthetic pathway was often accompanied with defects in plant growth and development depending on which gene was targeted. For the severely silenced *CCR* plants, phenotypic abnormalities with irregular vessels usually arise, including plant size reduction, delayed flowering, delayed senescence, retarded seed development, biomass yield reduction and compromised pathogen defense (De Meester et al., 2020; De Meester et al., 2018; Jones et al., 2001; Leplé et al., 2007; Van Acker et al., 2014; van der Rest et al., 2006; Vanholme et al., 2012; Xue et al., 2015; Zhou et al., 2010).

Firstly, *BnCCR* over-expression improved lodging resistance compared with WT, especially for *BnCCR1-2ox* (Figure 2; Figure S12). When *CCR1* was reintroduced into *A. thaliana ccr1* mutants under the control of the ProSNBE promoter, specific expression of *CCR1* in the protoxylem and metaxylem vessel cells showed a full recovery in vascular integrity (De Meester *et al*., 2018). The breaking-resistance of both *BnCCR1-2ox* and *BnCCR2-4ox* plants was greatly enhanced in comparison with WT, with larger effect in *BnCCR1-2ox* lines than in *BnCCR2-4ox* lines. These results imply an improved lodging resistance of *BnCCRox* lines due to better development and growth in both morphology and lignification of roots and stems, which provides significant potential in molecular breeding of rapeseed with enhanced lodging resistance through over-expressing *BnCCR* genes.

Secondly, *BnCCR* over-expression also modified leaf morphology. Our Mäule staining results indicated that rapeseed petiole xylem was exclusively composed of vascular bundles without interfascicular fibers, which could account for better development of leaf veins in *BnCCR1-2ox* plants, since vascular bundles contained higher proportion of G-lignin and *BnCCR1-2* was mainly involved in the biosynthesis of G- and H-lignins. In *Arabidopsis*, *CCR1* also mediated cell proliferation exit for leaf development, and *ccr1-4* mutant had a significantly reduced leaf and plant size compared with WT (Xue *et al*., 2015). However, *BnCCR2-4ox* plants showed less developed leaf vascular

bundles (Figure 4o; Figure S12j), which could possibly be resulted from two reasons: weakened G-unit synthesis (since *BnCCR2-4* overexpression mainly forced S-unit synthesis), and downregulated *BnCCR1* expression in leaves of *BnCCR2-4ox* plants (Figure S17b). Enhanced levels of ABA might also play a role in the alteration of leaf phenotypes of *BnCCRox* plants (Figure S13), as ABA plays important roles in plant growth and development (Cutler *et al*., 2010).

Thirdly, resistance of *BnCCRox* plants to *S. sclerotiorum* and UV-B was not improved, which was in confliction with traditional notion and our original expectation. There are many factors involved in plant disease resistance, such as the epidermal cuticle-wax layers, trichomes, lignified cell walls, phenolics, phytoalexins and pathogenesis-related proteins (Zhao *et al*., 2007). In the present study, although the lignin content was increased through *BnCCR* over-expression, the other important factors correlated to the plant resistance were not enhanced or even suppressed by flux competition between lignin pathway and flavonoid and other pathways, which could be reflected by the changes of flavonoid and glucosinolate metabolic profiles. Besides, decrease of epidermal wax layer was observed on leaves of *BnCCR1-2ox* plants compared with *BnCCR2-4ox* and WT (Figure S18). According to this study, sole over-expression of *CCR* genes in *B. napus* could not enhance resistance to *S. sclerotiorum* and UV-B, although *BnCCR2* subfamily could be sharply and intensively induced by *S. sclerotiorum* infection and UV-B irradiation.

BnCCR1 and _BnCCR2_ differentially affect plant development progress

During the progress of the growth and development of *BnCCRox* plants, the upper stem of *BnCCR1-2ox* plants at bolting stage was more easily to bend, but *BnCCR2-4ox* plants had no such case (Figure 2f; Figure S12a). As reported, S-lignin percentage in stems would gradually increase during plant growth process (Giordano *et al*., 2014; Tu *et al*., 2010). Mäule staining of stem cross sections in this study revealed similar trend (Figure S19), suggesting that S-lignin might play an important role for maturation and mechanical strength of stems. Kaur *et al*. (2012) found that the stem of *CAD*-downregulated *Nicotiana*

plants (ir-CAD) presented a rubbery phenomenon, and the S/G ratio was significantly reduced. Here the S/G ratio was also significantly decreased in *BnCCR1-2ox* plants (1.29 in WT, 0.68 in ox1-5, and 0.98 in ox1-12). Moreover, our results showed that in WT the S/G ratio in stem (1.29) was significantly higher than in root (0.49), which might be one factor contributing to the more flexible texture of roots compared with stems, although total lignin content was higher in root than in stem (Figure 4r and s). Lower percentage of S-units might contribute to a lower level of stiffness of the stem, together with the lower lignin content in the upper stem, which might be one reason of the bending phenomenon of *BnCCR1-2ox* at bolting stage. However, when *BnCCR1-2ox* plants entered flowering stage, the bending phenomenon disappeared, which might be due to increase in total lignin content and S-lignin percentage in stems (Figure S19). Relationship between S/G ratio and the texture of the plant stems was summarized in the Table S7. These results suggest that higher S/G ratio might contributes to stronger stiffness in plant stems, which is manifested during reproductive growth.

In this study, *BnCCR1-2ox* plants flowered distinctly later than WT and *BnCCR2-4ox* plants, implying that the function of Brassicaceae *CCR1* is also associated with plant development progress. Vermerris *et al*. (2002) reported that there was an evolutionarily conserved mechanism between cell wall biosynthesis and production of flowers. The delayed increase of S-lignin proportion, lowered stem stiffness and delayed stem maturation at bolting stage were reflections of delayed development progress and flowering in *BnCCR1-2ox* plants.

BnCCR1 and _BnCCR2_ exert different flux control on flavonoid pathway and lignin-derivative pathways in _B. napus_

In metabolic engineering, products, precursor steps as well as associated neighbor pathways would be affected via metabolic flux redirection. In lignin engineering, for example, significantly higher amounts of vanillin, ferulic acid,

p-coumaric acid, coniferaldehyde and syringaldehyde were released from the cell wall samples of *MtCAD1* mutants than the wild-type (Zhao *et al*., 2013). In the *C3'H* (Abdulrazzak *et al*., 2006) or *HCT* (Besseau *et al*., 2007) defect *Arabidopsis*, *C3H1*-downregulated maize (Fornalé *et al*., 2015), *CCR*-silenced tomato (van der Rest *et al*., 2006) and perennial ryegrass (Tu *et al*., 2010), the accumulation of flavonoids was significantly increased.

Besides enhancement of lignin monomers, our results also showed that both *BnCCR1-2* and *BnCCR2-4* over-expressors had significantly increased levels of various CCR-downstream pathway products when compared with WT, especially for sinapate esters (Figure 5; Table S4-S6), which could be caused by the enhanced expression levels of corresponding genes *CCR*, *F5H*, *COMT* and *CAD*. Moreover, *BnCCR2-4ox* plants had a stronger effect on the accumulation of sinapate esters in stems than *BnCCR1-2ox* plants, implying that the metabolic route related to BnCCR2 catabolism (mainly S-units synthesis) might be closer to sinapate ester pathway than BnCCR1 (Figure 5a; Figure 7).

More strikingly, many compounds synthesized in flavonoid pathway were significantly reduced in *BnCCRox* plants compared with WT. The dramatic reduction in flavonoids was theoretically caused by the reduced availability of *p*-coumaroyl-CoA precursor for CHS as *BnCCR* overexpression attracted more of this common precursor into lignin pathway (Figure 7). This kind of flux shift could be further evidenced on molecular level (Figure 6). Seed color degree, metabolic profile and gene expression profile all indicated that suppression impact on flavonoid pathway was greater in *BnCCR1-2ox* plants than in *BnCCR2-4ox* plants (Figures 3 and 6; Tables S4-S6). Higher flux control effect on flavonoid pathway by BnCCR1 than by BnCCR2 could result from the fact that the metabolic routes of BnCCR1 catabolism (mainly H- and G-units synthesis) were closer to flavonoid pathway than that of BnCCR2 (mainly S-unit synthesis) as suggested in Figure 7.

Brassica yellow-seed cultivars are superior to traditional black-seed cultivars featured by thinner seed coat, higher oil content, little seed coat pigments and lower crude fibers (Qu *et al*., 2013; Zhang *et al*., 2013). This study indicates

that downregulation of *CCR1* subfamily is a contribution factor of the decreased lignification in natural *Brassica* yellow seeds, while upregulation of *CCR2* subfamily could hardly compensate this effect (Figure S3-S6). *BnCCR1* and *BnCCR2* overexpressing seeds also showed yellow-seed phenotype with decreased seed coat pigments, and *BnCCR1* had much stronger effect than *BnCCR2*, implying that *CCR1* and *CCR2* in *Brassica* are differently associated with yellow-seed trait. Different from natural yellow seeds, *CCR*-overexpressing "yellow seeds" had increased lignins with no reduction in seed coat thickness (Figures 3 and 4t).

BnCCR1 and _BnCCR2_ play different roles in crosstalk between phenylpropanoid pathway and glucosinolate pathway

There were a few reports on crosstalk effect of glucosinolate pathway on phenylpropanoid pathway (Hemm *et al*., 2003; Kim *et al*., 2015; Kim *et al*., 2020). In *Arabidopsis*, Kim *et al*. (2015) found that the accumulation of phenylpropanoids were significantly suppressed in *ref5-1* mutant, and *REF5* was proved to encode CYP83B1 which was involved in biosynthesis of indole glucosinolates. Defect of phenylpropanoids deposition was also detected in *Arabidopsis ref2* mutant, as *REF2* encoded CYP83A1 which played a role in aliphatic glucosinolate pathway (Hemm *et al*., 2003). In low-lignin *c4h*, *4cl1*, *ccoaomt1* and *ccr1* mutants of *Arabidopsis*, transcripts of some glucosinolate biosynthesis genes were more abundant (Vanholme *et al*., 2012). However, to date there is no systemic study on crosstalk effect of phenylpropanoid pathway on glucosinolate pathway.

In present study, the aliphatic glucosinolates were significantly increased in *BnCCR1-2ox* (Table S4), which could result from upregulated expression of *MYB28*, *MYB29*, *CYP79F1*, *CYP83A1*, *AOP2* and *GSL* in the leaves of transgenic plants (Figure 6). Among them, the expression of *MYB29*, *CYP79F1* and *GSL* could almost only be detected in *BnCCR1-2ox*, not in WT. Reasonably, the undetectable *MYB29* expression and extremely lower expression of *MYB51*, *MYB122*, *AOP2*, *CYP79B2*, *ST5a* and *IGMT1* in *BnCCR2-4ox* plants could be responsible for the decrease of glucosinolate content. Because the WT material ZS10 of this study was a "double-low" (low

erucic acid, low glucosinolates) commercial cultivar, the low proportion of indole and aromatic glucosinolates in WT and the limited change of indole and aromatic glucosinolates in *BnCCR*-overexpressing plants might be caused by breeding impairment of respective biosynthesis pathways of these two types of glucosinolates. If a “double-high” stock was used as WT for *BnCCR* transformation, the effect on indole and aromatic glucosinolates deposition might not be so mild. Taken together, both *BnCCR1-2* and *BnCCR2-4* distinctly affect glucosinolate biosynthesis, but have divergent or almost opposite effects.

Crosstalk effect of glucosinolate pathway on phenylpropanoid pathway could be linked through PAL degradation that mediated by Med5-KFBs-dependent manner (Kim *et al*., 2020). However, what mechanism is involved in change of glucosinolate biosynthesis by manipulating phenylpropanoid genes, such as *CCR*, needs to be clarified. Our qRT-PCR results indicate that at least transcription regulation is involved, but whether mediator-mediated protein degradation in glucosinolate pathway is also involved deserves future study.

This study provides systemic molecular and functional dissection of *B. napus CCR*s and *CCR1-CCR2* functional divergence in Brassicaceae, which will promote the advancement of *CCR*-related mechanism and traits improvement of *Brassica* crops.

Methods

See Supplementary Methods.

Author contributions

Y.C., J.L. and N.Y. designed the study; N.Y., B.L., X.L. and Y.X. performed the experiments; Y.C. did molecular and bioinformatic analysis, N.Y., J.L., M.C., K.L., L.W. and Y.L. analyzed or evaluated the results; J.L. and R.W. provided some *Brassica* materials. N.Y. and Y.C. performed final analysis and wrote the article.

Acknowledgements

We thank Prof Xuekuan Zhang for providing Zhongshuang 10 seeds, Prof Wei Qian for providing the *S. sclerotiorum* source strain, Prof Ningjia He, Dr. Guangyu Ding and Dr. Shiyao Liu for assistance on GC-MS measurements. This research was supported by National Natural Science Foundation of China (31871549, 32001579, 31830067 and 31171177), National Key R&D Program of China (2016YFD0100506), Special financial aid to post-doctor research fellow of Chongqing (XmT2018057), “111” Project (B12006), and Young Eagles Program of Chongqing Municipal Commission of Education (CY200215).

Conflict of interest

The authors declare no conflict of interest.

Supporting information

Figure S1 Southern blot detection of *CCR* subfamily genes in *B. napus*, *B. rapa* and *B. oleracea*.

(a) *CCR1* subfamily genes detection.

(b) *CCR2* subfamily genes detection.

The total genomic DNA was fully digested with *Dra*I, *Eco*RI, *Eco*RV, *Hin*dIII and *Xba*I, respectively.

Figure S2 Multi-alignment indicates that *Brassica* CCRs contain complete structural features as those in model plants *A. thaliana* and popular.

The accession numbers of *Brassica* and *A. thaliana* CCRs are the same as in Figure 1, while the accession number of *Populus tremuloides* CCR (PtCCR) is AAF43141.1. Green bars, NADP binding motifs; Yellow bars, substrate binding motifs; Red boxes, conserved catalytic activity motifs of CCR.

Figure S3 Overall expression patterns of *CCR1*-subfamily and *CCR2*-subfamily show distinct organ-specificity and difference between black and yellow seeds in *B. napus*, *B. rapa* and *B. oleracea*.

5B, 09L597 and 09L598 are black-seed stocks, while 09L587, 09L600 and

09L599 are yellow-seed stocks, of *B. napus*, *B. rapa* and *B. oleracea*, respectively. The value (SEM in brackets) above the sRT-PCR band represents the relative expression level of qRT-PCR result. The expression level in root is set as 1.000 for quantification of other organs. Ro, roots; Hy, Hypocotyl; YS, young stems; OS, old stems; Co, cotyledons; Le, leaves; SP, silique pericarp; Fl, flowers; Bu, buds; 15D-55D, seeds of the corresponding days after pollination.

Figure S4 Expression patterns of *CCR1*-genes and *CCR2*-genes show distinct organ-specificity and difference between black and yellow seeds in *B. napus*.
5B and 09L587 are black- and yellow-seed stocks, respectively. The value (SEM in brackets) above the sRT-PCR band represents the relative expression level of qRT-PCR result. The expression level in root is set as 1.000 for quantification of other organs. Ro, roots; Hy, Hypocotyl; YS, young stems; OS, old stems; Co, cotyledons; Le, leaves; SP, silique pericarp; Fl, flowers; Bu, buds; 15D-55D, seeds of the corresponding days after pollination.

Figure S5 Expression patterns of *CCR1*-genes and *CCR2*-genes show distinct organ-specificity and difference between black and yellow seeds in *B. rapa*.
09L597 and 09L600 are black- and yellow-seed stocks, respectively. The value (SEM in brackets) above the sRT-PCR band represents the relative expression level of qRT-PCR result. The expression level in root of 09L597 is set as 1.000 for quantification of other organs. Ro, roots; Hy, Hypocotyl; YS, young stems; OS, old stems; Co, cotyledons; Le, leaves; SP, silique pericarp; Fl, flowers; Bu, buds; 15D-55D, seeds of the corresponding days after pollination.

Figure S6 Expression patterns of *CCR1*-genes and *CCR2*-genes show distinct organ-specificity and difference between black and yellow seeds in *B. oleracea.*
09L598 and 09L599 are black- and yellow-seed stocks, respectively. The value (SEM in brackets) above the sRT-PCR band represents the relative expression level of qRT-PCR result. The expression level in root is set as 1.000 for quantification of other organs. Ro, roots; Hy, Hypocotyl; YS, young stems; OS, old stems; Co, cotyledons; Le, leaves; SP, silique pericarp; Fl,

flowers; Bu, buds; 15D-55D, seeds of the corresponding days after pollination.

Figure S7 Overall expression of *BnCCR1*-subfamily and *BnCCR2*-subfamily distinctly respond to various stresses in *B. napus* seedlings.

The value (SEM in brackets) above the sRT-PCR band represents the relative expression level of qRT-PCR result. The expression level in the first sample is set as 1.000 for quantification of other samples. m, minutes; D&HT, drought & high temperature.

Figure S8 *BnCCR1*-genes and *BnCCR2*-genes distinctly respond to various stresses in *B. napus* seedlings.

The value (SEM in brackets) above the sRT-PCR band represents the relative expression level of qRT-PCR result. The expression level in the first sample is set as 1.000 for quantification of other samples. m, minutes; D&HT, drought & high temperature.

Figure S9 Basta-resistance, GUS-staining and PCR determination of transgenic lines.

Figure S10 qRT-PCR shows distinct upregulation of the target genes in respective T2 lines of *BnCCR1-2ox* and *BnCCR2-4ox*.

Error bars indicate SD of 3 biological replicates.

Figure S11 Multiple agronomic traits are significantly modified in *BnCCR1-2ox* and *BnCCR2-4ox* lines.

(a) to (d) Leaf area (a), leaf length (b), petiole width (c) and chlorophyll content (d) of the fifth and sixth leaves (the most robust leaves) during 9 to 12 leaf-stages.

(e) Diameter of the middle stem at early flowering stage.

(f) Anti-breaking strength of the middle stem at harvest stage after drying.

(g) and (h) The length and width of the siliques at mature stage.

(i) Number of primary branches.

(j) Plant height at mature stage.

(k) Silique number per plant.

(l) Seed yield per plant.

Data represent means ± SD of at least five biological replicates. Different letters above the bars indicate statistically significant differences (one-way ANOVA, $P < 0.05$, Duncan's test).

Figure S12 *BnCCR1-2ox* and *BnCCR2-4ox* lines show different growth behaviors and leaf vein strengths.

(a) Delay of bolting and flowering was observed in *BnCCR1-2ox* plants when compared with WT and *BnCCR1-2ox*, and upper stems of *BnCCR1-2ox* at late bolting stage are softer than normal ones and showed a bending phenomenon.

(b) After flowering, both *BnCCR1-2ox* and *BnCCR2-4ox* lines displayed a better lodging resistance than WT, especially for *BnCCR1-2ox* lines.

(c) and (d) Compared with WT and *BnCCR1-2ox*, leaves of *BnCCR2-4ox* seedlings in the morning (about 8:00) have normal angles (c), but showed a rolling-over phenomenon in the afternoon (about 3:00) under strong sunshine (d).

(e) to (f) At vegetative stage, the strongest leaves of *BnCCR1-2ox* and *BnCCR2-4ox* were distinctly larger than WT, both had similar effect on leaf blade growth, but *BnCCR1-2ox* had larger effect on petiole-vein growth than *BnCCR2-4ox*.

(g) to (j) Though visual observation of petiole-vein system of both *BnCCR1-2ox* and *BnCCR2-4ox* were larger than WT ([g] and [h]), phloroglucinol-HCl staining showed that petiole-vein lignification was strengthened only in *BnCCR1-2ox* plants while weakened in *BnCCR2-4ox* plants ([i] and [j]).

Figure S13 ABA content is upregulated in leaves of *BnCCR1-2ox* and *BnCCR2-4ox* lines.

Data represent means ± SD of at least 3 biological replicates. Different letters above the bars indicate statistically significant differences (one-way ANOVA, $P < 0.05$, Duncan's test).

Figure S14 Plants of both *BnCCR1-2ox* and *BnCCR2-4ox* do not show enhanced resistance to *S. sclerotiorum* and UV-B.

(a) to (d) Lesions on detached leaves and stems after 48 h and 72 h of inoculation respectively.

(e) and (f) Lesion areas on leaves and lesion lengths on stems respectively. Data represent means ± SD of at least 3 biological replicates. Different letters above the bars indicate statistically significant differences (one-way ANOVA, $P < 0.05$, Duncan's test).

(g) and (h) Pot seedlings before UV-B treatment and 1 week after 1-h UV-B treatment respectively.

Figure S15 GC-MS chromatograms show different changes of monolignol proportions in *BnCCR1-2ox* and *BnCCR2-4ox* lines.

IS, Internal standard tetracosane; H1, H2, G1, G2, S1 and S2 represent the isomers of the corresponding H-, G- and S-lignin monomers.

Figure S16 Contents of cellulose and hemicellulose in the stems of *BnCCR1-2ox* and *BnCCR2-4ox* lines are not changed based on NIRS detection.

Figure S17 *BnCCR1* expression is obviously altered in *BnCCR2-4ox* lines, whereas *BnCCR2* expression has little change in *BnCCR1-2ox* lines.

(a) to (d) *BnCCR1* expression is upregulated in stems, petioles and seeds, while downregulated in leaves, of *BnCCR2-4ox* lines.

(e) to (h) *BnCCR2* expression is almost not changed in stems, leaves, petioles and seeds of *BnCCR1-2ox* lines.

Figure S18 Leaf surfaces of *BnCCR1-2ox* and *BnCCR2-4ox* plants are less flat with decreased wax deposition than WT.

(a) to (c): Electron microscopy observation shows that leaf surface cells of *BnCCR1-2ox* and *BnCCR2-4ox* plants are more prominent than WT. Bar = 100 μm.

(d) to (f): Electron microscopy observation shows that leaf epidermal wax crystals of *BnCCR1-2ox* and *BnCCR2-4ox* plants are less than WT. Bar = 10 μm.

Figure S19 Mäule staining of stem sections indicates a trend of increase of S-type lignins during developmental process in *B. napus*.

(a) Middle-upper part of the stem at early flowering stage.

(b) Middle-lower part of the stem at early flowering stage.

(c) Middle-upper part of the stem at mature stage.

Table S1 Identity parameters of *CCR1*-subfamily and *CCR2*-subfamily genes from *B. napus* and its parental species *B. oleracea* and *B. rapa*.

Table S2 cDNA and gDNA basic parameters of *Brassica CCR1* and *CCR2* subfamily genes cloned in this study.

Table S3 Basic parameters and important features of *Brassica* CCR1 and CCR2 proteins.

Table S4 Contents of major soluble secondary metabolites differentially accumulated in stems and leaves of ox1-5 and ox2-16 compared with WT as revealed by UPLC-HESI-MS/MS.

Table S5 Contents of major soluble secondary metabolites differentially accumulated in 30DAP seeds of ox1-5 and ox2-16 compared with WT as revealed by UPLC-HESI-MS/MS.

Table S6 Contents of major soluble secondary metabolites differentially accumulated in petioles of ox1-5 and ox2-16 compared with WT as revealed by UPLC-HESI-MS/MS.

Table S7 S/G ratio of stem lignin, stem stiffness, and plant phenotype of different angiosperm species.

Table S8 Primers used in this study.

Data Set Data of statistical analysis in this study (Student's t-test and ANOVA).

References

Abdulrazzak, N., Pollet, B., Ehlting, J., Larsen, K., Asnaghi, C., Ronseau, S., Proux, C., Erhardt, M., Seltzer, V., Renou, J.P., Ullmann, P., Pauly, M., Lapierre, C. and Werck-Reichhart, D. (2006) A coumaroyl-ester-3-hydroxylase insertion mutant reveals the existence of nonredundant meta-hydroxylation pathways and essential roles for phenolic precursors in cell expansion and plant growth. *Plant physiol.* **140**, 30-48.

Acreche, M.M. and Slafer, G.A. (2011) Lodging yield penalties as affected by breeding in Mediterranean wheats. *Field Crop Res.* **122**, 40-48.

Bart, R.S., Chern, M., Vega-Sanchez, M.E., Canlas, P. and Ronald, P.C. (2010) Rice *Snl6*, a *Cinnamoyl-CoA Reductase-Like* gene family member, is required for *nh1*-mediated immunity to *Xanthomonas oryzae pv. oryzae*. *Plos Genet.* **6**, e1001123.

Baucher, M., Halpin, C., Petit-Conil, M. and Boerjan, W. (2003) Lignin: Genetic engineering and impact on pulping. *Crit. Rev. Biochem. Mol.* **38**, 305-350.

Baucher, M., Monties, B., Van Montagu, M. and Boerjan, W. (1998) Biosynthesis and genetic engineering of lignin. *Crit. Rev. Plant Sci.* **17**, 125-197.

Berry, P.M. (2018) Lodging Resistance in Cereals. In: Meyers R. (eds) Encyclopedia of Sustainability Science and Technology. *Springer* **New York**, NY. https://doi.org/10.1007/1978-1001-4939-2493-1006_1228-1003.

Berry, P.M. and Spink, J. (2012) Predicting yield losses caused by lodging in wheat. *Field Crop Res.* **137**, 19-26.

Berthet, S., Demont-Caulet, N., Pollet, B., Bidzinski, P., Cezard, L., Le Bris, P., Borrega, N., Herve, J., Blondet, E., Balzergue, S., Lapierre, C. and Jouanin, L. (2011) Disruption of *laccase4* and *17* results in tissue-specific alterations to lignification of *Arabidopsis thaliana* stems. *Plant Cell*, **23**, 1124-1137.

Besseau, S., Hoffmann, L., Geoffroy, P., Lapierre, C., Pollet, B. and Legrand, M. (2007) Flavonoid accumulation in *Arabidopsis* repressed in lignin synthesis affects auxin transport and plant growth. *Plant Cell*, **19**, 148-162.

Caño-Delgado, A., Penfield, S., Smith, C., Catley, M. and Bevan, M. (2003) Reduced cellulose synthesis invokes lignification and defense responses in *Arabidopsis thaliana*. *Plant J.* **34**, 351-362.

Chabannes, M., Barakate, A., Lapierre, C., Marita, J.M., Ralph, J., Pean, M., Danoun, S., Halpin, C., Grima-Pettenati, J. and Boudet, A.M. (2001) Strong decrease in lignin content without significant alteration of plant development is induced by simultaneous down-regulation of *cinnamoyl CoA reductase* (*CCR*) and *cinnamyl alcohol dehydrogenase* (*CAD*) in tobacco plants. *Plant J.* **28**, 257-270.

Chantreau, M., Portelette, A., Dauwe, R., Kiyoto, S., Cronier, D., Morreel, K., Arribat, S., Neutelings, G., Chabi, M., Boerjan, W., Yoshinaga, A., Mesnard, F., Grec, S., Chabbert, B. and Hawkins, S. (2014) Ectopic lignification in the flax lignified bast *fiber1* mutant stem is associated with tissue-specific modifications in gene expression and cell wall composition. *Plant Cell*, **26**, 4462-4482.

Chao, N., Jiang, W.T., Wang, X.C., Jiang, X.N. and Gai, Y. (2019) Novel motif is capable of

determining CCR and CCR-like proteins based on the divergence of CCRs in plants. *Tree Physiol.* **39**, 2019-2026.

Costa, S. and Dolan, L. (2003) Epidermal patterning genes are active during embryogenesis in *Arabidopsis*. *Development* **130**, 2893-2901.

Cutler, S.R., Rodriguez, P.L., Finkelstein, R.R. and Abrams, S.R. (2010) Abscisic acid: emergence of a core signaling network. *Annu. Rev. Plant Biol.* **61**, 651-679.

Dauwe, R., Morreel, K., Goeminne, G., Gielen, B., Rohde, A., Van Beeumen, J., Ralph, J., Boudet, A.M., Kopka, J., Rochange, S.F., Halpin, C., Messens, E. and Boerjan, W. (2007) Molecular phenotyping of lignin-modified tobacco reveals associated changes in cell-wall metabolism, primary metabolism, stress metabolism and photorespiration. *Plant J.* **52**, 263-285.

De Meester, B., Calderón, B.M., de Vries, L., Pollier, J., Goeminne, G., Van Doorsselaere, J., Chen, M., Ralph, J., Vanholme, R. and Boerjan, W. (2020) Tailoring poplar lignin without yield penalty by combining a null and haploinsufficient *CINNAMOYL-CoA REDUCTASE2* allele. *Nat Commun.* **11**, 1-13.

De Meester, B., de Vries, L., Ozparpucu, M., Gierlinger, N., Corneillie, S., Pallidis, A., Goeminne, G., Morreel, K., De Bruyne, M., De Rycke, R., Vanholme, R. and Boerjan, W. (2018) Vessel-specific reintroduction of *CINNAMOYL-COA REDUCTASE1* (*CCR1*) in dwarfed ccr1 mutants restores vessel and xylary fiber integrity and increases biomass. *Plant physiol.* **176**, 611-633.

del Río, L.E., Bradley, C.A., Henson, R.A., Endres, G.J., Hanson, B.K., Mckay, K., Halvorson, M., Porter, P.M., Le Gare, D.G. and Lamey, H.A. (2007) Impact of *Sclerotinia* stem rot on yield of canola. *Plant Dis.* **91**, 191-194.

Ding, Y.J., Mei, J.Q., Liu, Y., Wang, L., Li, Y.H., Wan, H.F., Li, J.N. and Qian, W. (2015) Transfer of *sclerotinia* stem rot resistance from wild *Brassica oleracea* into *B-rapa*. *Mol. Breeding,* **35**.

Escamilla-Treviño, L.L., Shen, H., Uppalapati, S.R., Ray, T., Tang, Y.H., Hernandez, T., Yin, Y.B., Xu, Y. and Dixon, R.A. (2010) Switchgrass (*Panicum virgatum*) possesses a divergent family of cinnamoyl CoA reductases with distinct biochemical properties. *New Phytol.* **185**, 143-155.

Fan, B., Hu, S., Lu, H. and Jiang, X. (2006) Soluble prokaryotic expression of *4-coumarate: coenzyme A ligase* from *Populus tomentosa* and enzyme activity of recombinant 4CL1. *Journal-Beijing Forestry University-Chinese Edition-* **28**, 1.

Fornalé, S., Rencoret, J., Garcia-Calvo, L., Capellades, M., Encina, A., Santiago, R., Rigau, J., Gutierrez, A., del Rio, J.C. and Caparros-Ruiz, D. (2015) Cell wall modifications triggered by the down-regulation of *Coumarate 3-hydroxylase-1* in maize. *Plant Sci.* **236**, 272-282.

Giordano, A., Liu, Z.Q., Panter, S.N., Dimech, A.M., Shang, Y.J., Wijesinghe, H., Fulgueras, K., Ran, Y.D., Mouradov, A., Rochfort, S., Patron, N.J. and Spangenberg, G.C. (2014) Reduced lignin content and altered lignin composition in the warm season forage grass *Paspalum dilatatum* by down-regulation of a *Cinnamoyl CoA Reductase* Gene. *Transgenic Res.* **23**, 503-517.

Goujon, T., Ferret, V., Mila, I., Pollet, B., Ruel, K., Burlat, V., Joseleau, J.P., Barriere, Y., Lapierre, C. and Jouanin, L. (2003) Down-regulation of the *AtCCR1* gene in *Arabidopsis thaliana*: effects on phenotype, lignins and cell wall degradability. *Planta*, **217**, 218-228.

Hemm, M.R., Ruegger, M.O. and Chapple, C. (2003) The *Arabidopsis ref2* mutant is defective

in the gene encoding CYP83A1 and shows both phenylpropanoid and glucosinolate phenotypes. *Plant Cell*, **15**, 179-194.

Hoffmann, L., Besseau, S., Geoffroy, P., Ritzenthaler, C., Meyer, D., Lapierre, C., Pollet, B. and Legrand, M. (2004) Silencing of hydroxycinnamoyl-coenzyme A shikimate/quinate hydroxycinnamoyltransferase affects phenylpropanoid biosynthesis. *Plant Cell*, **16**, 1446-1465.

Huang, J.L., Gu, M., Lai, Z.B., Fan, B.F., Shi, K., Zhou, Y.H., Yu, J.Q. and Chen, Z.X. (2010) Functional analysis of the *Arabidopsis PAL* gene family in plant growth, development, and response to environmental stress. *Plant physiol.* **153**, 1526-1538.

Jones, L., Ennos, A.R. and Turner, S.R. (2001) Cloning and characterization of irregular xylem4 (*irx4*): a severely lignin-deficient mutant of *Arabidopsis*. *Plant J.* **26**, 205-216.

Kaur, H., Shaker, K., Heinzel, N., Ralph, J., Galis, I. and Baldwin, I.T. (2012) Environmental stresses of field growth allow cinnamyl alcohol dehydrogenase-deficient *nicotiana attenuata* plants to compensate for their structural deficiencies. *Plant physiol.* **159**, 1545-1570.

Kawasaki, T., Koita, H., Nakatsubo, T., Hasegawa, K., Wakabayashi, K., Takahashi, H., Urnemura, K., Urnezawa, T. and Shimamoto, K. (2006) Cinnamoyl-CoA reductase, a key enzyme in lignin biosynthesis, is an effector of small GTPase Rac in defense signaling in rice. *P. Nat.l Acad. Sci. USA* **103**, 230-235.

Kendall, S.L., Holmes, H., White, C.A., Clarke, S.M. and Berry, P.M. (2017) Quantifying lodging-induced yield losses in oilseed rape. *Field Crop Res.* **211**, 106-113.

Kim, J.I., Dolan, W.L., Anderson, N.A. and Chapple, C. (2015) Indole glucosinolate biosynthesis limits phenylpropanoid accumulation in *Arabidopsis thaliana*. *Plant Cell*, **27**, 1529-1546.

Kim, J.I., Zhang, X., Pascuzzi, P.E., Liu, C.J. and Chapple, C. (2020) Glucosinolate and phenylpropanoid biosynthesis are linked by proteasome-dependent degradation of PAL. *New Phytol.* **225**, 154-168.

Ko, J.K., Ximenes, E., Kim, Y. and Ladisch, M.R. (2015) Adsorption of enzyme onto lignins of liquid hot water pretreated hardwoods. *Biotechnol. Bioeng.* **112**, 447-456.

Koch, S., Dunker, S., Kleinhenz, B., Rohrig, M. and von Tiedemann, A. (2007) Crop loss-related forecasting model for *Sclerotinia* stem rot in winter oilseed rape. *Phytopathology*, **97**, 1186-1194.

Labeeuw, L., Martone, P.T., Boucher, Y. and Case, R.J. (2015) Ancient origin of the biosynthesis of lignin precursors. *Biol. Direct*, **10**. 23.

Lacombe, E., Hawkins, S., VanDoorsselaere, J., Piquemal, J., Goffner, D., Poeydomenge, O., Boudet, A.M. and GrimaPettenati, J. (1997) Cinnamoyl CoA reductase, the first committed enzyme of the lignin branch biosynthetic pathway: cloning, expression and phylogenetic relationships. *Plant J.* **11**, 429-441.

Lauvergeat, V., Lacomme, C., Lacombe, E., Lasserre, E., Roby, D. and Grima-Pettenati, J. (2001) Two cinnamoyl-CoA reductase (CCR) genes from *Arabidopsis thaliana* are differentially expressed during development and in response to infection with pathogenic bacteria. *Phytochemistry*, **57**, 1187-1195.

Lee, M.H., Jeon, H.S., Kim, S.H., Chung, J.H., Roppolo, D., Lee, H.J., Cho, H.J., Tobimatsu, Y., Ralph, J. and Park, O.K. (2019) Lignin-based barrier restricts pathogens to the infection site and confers resistance in plants. *Embo. J.* **38**, e101948.

Leplé, J.C., Dauwe, R., Morreel, K., Storme, V., Lapierre, C., Pollet, B., Naumann, A., Kang, K.Y., Kim, H., Ruel, K., Lefebvre, A., Joseleau, J.P., Grima-Pettenati, J., De Rycke, R., Andersson-Gunneras, S., Erban, A., Fehrle, I., Petit-Conil, M., Kopka, J., Polle, A., Messens, E., Sundberg, B., Mansfield, S.D., Ralph, J., Pilate, G. and Boerjan, W. (2007) Downregulation of cinnamoyl-coenzyme a reductase in poplar: Multiple-level phenotyping reveals effects on cell wall polymer metabolism and structure. *Plant Cell*, **19**, 3669-3691.

Li, X., Bonawitz, N.D., Weng, J.K. and Chapple, C. (2010) The growth reduction associated with repressed lignin biosynthesis in *Arabidopsis thaliana* is independent of flavonoids. *Plant Cell*, **22**, 1620-1632.

Li, X., Weng, J.K. and Chapple, C. (2008) Improvement of biomass through lignin modification. *Plant J.* **54**, 569-581.

Liu, C., Wang, J.L., Huang, T.D., Wang, F., Yuan, F., Cheng, X.M., Zhang, Y., Shi, S.W., Wu, J.S. and Liu, K.D. (2010) A missense mutation in the VHYNP motif of a DELLA protein causes a semi-dwarf mutant phenotype in *Brassica napus*. *Theor. Appl. Genet.* **121**, 249-258.

Ma, Q.H. (2009) The expression of *caffeic acid 3-O-methyltransferase* in two wheat genotypes differing in lodging resistance. *J. Exp. Bot.* **60**, 2763-2771.

Pan, L.G., Assirelli, A., Suardi, A., Civitarese, V., Del Giudice, A., Costa, C. and Santangelo, E. (2012) The harvest of oilseed rape (*Brassica napus* L.): The effective yield losses at on-farm scale in the Italian area. *Biomass Bioenerg.* **46**, 453-458.

Patten, A.M., Cardenas, C.L., Cochrane, F.C., Laskar, D.D., Bedgar, D.L., Davin, L.B. and Lewis, N.G. (2005) Reassessment of effects on lignification and vascular development in the *irx4 Arabidopsis* mutant. *Phytochemistry*, **66**, 2092-2107.

Peng, D.L., Chen, X.G., Yin, Y.P., Lu, K.L., Yang, W.B., Tang, Y.H. and Wang, Z.L. (2014) Lodging resistance of winter wheat (*Triticum aestivum* L.): Lignin accumulation and its related enzymes activities due to the application of paclobutrazol or gibberellin acid. *Field Crop Res.* **157**, 1-7.

Piquemal, J., Lapierre, C., Myton, K., O'Connell, A., Schuch, W., Grima-Pettenati, J. and Boudet, A.M. (1998) Down-regulation of cinnamoyl-CoA reductase induces significant changes of lignin profiles in transgenic tobacco plants. *Plant J.* **13**, 71-83.

Prashant, S., Sunita, M.S., Pramod, S., Gupta, R.K., Kumar, S.A., Karumanchi, S.R., Rawal, S.K. and Kishor, P.B.K. (2011) Down-regulation of *Leucaena leucocephala cinnamoyl CoA reductase (LlCCR*) gene induces significant changes in phenotype, soluble phenolic pools and lignin in transgenic tobacco. *Plant Cell Rep.* **30**, 2215-2231.

Qu, C.M., Fu, F.Y., Lu, K., Zhang, K., Wang, R., Xu, X.F., Wang, M., Lu, J.X., Wan, H.F., Tang, Z.L. and Li, J.N. (2013) Differential accumulation of phenolic compounds and expression of related genes in black- and yellow-seeded *Brassica napus*. *J. Exp. Bot.* **64**, 2885-2898.

Ragauskas, A.J., Williams, C.K., Davison, B.H., Britovsek, G., Cairney, J., Eckert, C.A., Frederick, W.J., Hallett, J.P., Leak, D.J., Liotta, C.L., Mielenz, J.R., Murphy, R., Templer, R. and Tschaplinski, T. (2006) The path forward for biofuels and biomaterials. *Science*, **311**, 484-489.

Ruel, K., Berrio-Sierra, J., Derikvand, M.M., Pollet, B., Thevenin, J., Lapierre, C., Jouanin, L. and Joseleau, J.P. (2009) Impact of *CCR1* silencing on the assembly of lignified secondary walls in *Arabidopsis thaliana*. *New Phytol.* **184**, 99-113.

Tamasloukht, B., Lam, M.S.J.W.Q., Martinez, Y., Tozo, K., Barbier, O., Jourda, C., Jauneau, A., Borderies, G., Balzergue, S., Renou, J.P., Huguet, S., Martinant, J.P., Tatout, C., Lapierre, C., Barriere, Y., Goffner, D. and Pichon, M. (2011) Characterization of a *cinnamoyl-CoA reductase 1* (*CCR1*) mutant in maize: effects on lignification, fibre development, and global gene expression. *J. Exp. Bot.* **62**, 3837-3848.

Thévenin, J., Pollet, B., Letarnec, B., Saulnier, L., Gissot, L., Maia-Grondard, A., Lapierre, C. and Jouanin, L. (2011) The simultaneous repression of *CCR* and *CAD*, two enzymes of the lignin biosynthetic pathway, results in sterility and dwarfism in *Arabidopsis thaliana*. *Mol. plant*, **4**, 70-82.

Tongyan, W., Lingqin, X. and Xueju, Y. (2002) Study on the correlations between the components of the plant height and the yield and other traits of wheat. *Journal of Agricultural University of Hebei (China)*, **25**, 10-12,18.

Tu, Y., Rochfort, S., Liu, Z.Q., Ran, Y.D., Griffith, M., Badenhorst, P., Louie, G.V., Bowman, M.E., Smith, K.F., Noel, J.P., Mouradov, A. and Spangenberg, G. (2010) Functional Analyses of *Caffeic Acid O-Methyltransferase* and *Cinnamoyl-CoA-Reductase* Genes from Perennial Ryegrass *(Lolium perenne*). *Plant Cell*, **22**, 3357-3373.

Van Acker, R., Leple, J.C., Aerts, D., Storme, V., Goeminne, G., Ivens, B., Legee, F., Lapierre, C., Piens, K., Van Montagu, M.C.E., Santoro, N., Foster, C.E., Ralph, J., Soetaert, W., Pilate, G. and Boerjan, W. (2014) Improved saccharification and ethanol yield from field-grown transgenic poplar deficient in cinnamoyl-CoA reductase. *P. Natl. Acad .Sci. USA* **111**, 845-850.

van der Rest, B., Danoun, S., Boudet, A.M. and Rochange, S.F. (2006) Down-regulation of *cinnamoyl-CoA reductase* in tomato (*Solanum lycopersicum* L.) induces dramatic changes in soluble phenolic pools. *J. Exp. Bot.* **57**, 1399-1411.

Vanholme, R., Demedts, B., Morreel, K., Ralph, J. and Boerjan, W. (2010) Lignin biosynthesis and structure. *Plant physiol.* **153**, 895-905.

Vanholme, R., Storme, V., Vanholme, B., Sundin, L., Christensen, J.H., Goeminne, G., Halpin, C., Rohde, A., Morreel, K. and Boerjan, W. (2012) A systems biology view of responses to lignin biosynthesis perturbations in *Arabidopsis*. *Plant Cell*, **24**, 3506-3529.

Vermerris, W., Thompson, K.J., McIntyre, L.M. and Axtell, J.D. (2002) Evidence for an evolutionarily conserved interaction between cell wall biosynthesis and flowering in maize and sorghum. *BMC. Evol. Biol.* **2**, 1-8.

Wagner, A., Tobimatsu, Y., Goeminne, G., Phillips, L., Flint, H., Steward, D., Torr, K., Donaldson, L., Boerjan, W. and Ralph, J. (2013) Suppression of *CCR* impacts metabolite profile and cell wall composition in *Pinus radiata* tracheary elements. *Plant Mol. Biol.* **81**, 105-117.

Weng, J.K. and Chapple, C. (2010) The origin and evolution of lignin biosynthesis. *New Phytol.* **187**, 273-285.

Weng, J.K., Mo, H.P. and Chapple, C. (2010) Over-expression of *F5H* in *COMT*-deficient *Arabidopsis* leads to enrichment of an unusual lignin and disruption of pollen wall formation. *Plant J.* **64**, 898-911.

Xue, J.S., Luo, D.X., Xu, D.Y., Zeng, M.H., Cui, X.F., Li, L.G. and Huang, H. (2015) CCR1, an enzyme required for lignin biosynthesis in *Arabidopsis*, mediates cell proliferation exit for leaf development. *Plant J.* **83**, 375-387.

Zhang, G.P., Chen, J.X. and Bull, D.A. (2001) The effects of timing of N application and plant growth regulators on morphogenesis and yield formation in wheat. *Plant Growth Regul.* **35**, 239-245.

Zhang, K., Lu, K., Qu, C.M., Liang, Y., Wang, R., Chai, Y.R. and Li, J.N. (2013) gene silencing of *BnTT10* family genes causes retarded pigmentation and lignin reduction in the seed coat of *Brassica napus*. *Plos One*, **8**.

Zhang, W.B., Wei, R., Chen, S., Jiang, J., Li, H.Y., Huang, H.J., Yang, G., Wang, S., Wei, H.R. and Liu, G.F. (2015) Functional characterization of *CCR* in birch (*Betula platyphylla* x *Betula pendula*) through overexpression and suppression analysis. *Physiol. Plantarum*, **154**, 283-296.

Zhao, J., Wang, J., An, L., Doerge, R., Chen, Z.J., Grau, C.R., Meng, J. and Osborn, T.C. (2007) Analysis of gene expression profiles in response to *Sclerotinia sclerotiorum* in *Brassica napus*. *Planta*, **227**, 13-24.

Zhao, Q., Tobimatsu, Y., Zhou, R., Pattathil, S., Gallego-Giraldo, L., Fu, C., Jackson, L.A., Hahn, M.G., Kim, H., Chen, F., Ralph, J. and Dixon, R.A. (2013) Loss of function of *cinnamyl alcohol dehydrogenase 1* leads to unconventional lignin and a temperature-sensitive growth defect in *Medicago truncatula*. *P. Natl. Acad. Sci. USA*, **110**, 13660-13665.

Zhou, R., Jackson, L., Shadle, G., Nakashima, J., Temple, S., Chen, F. and Dixon, R.A. (2010) Distinct cinnamoyl CoA reductases involved in parallel routes to lignin in *Medicago truncatula*. *P. Natl. Acad. Sci. USA*, **107**, 17803-17808.

Figure legends

Figure 1 Phylogenetic analysis of CCR refseq_proteins from representative whole-genome-sequenced Malvids species including *B. napus, B. rapa* and *B. oleracea*.

Latin name, refseq_protein name and accession number are provided for each sequence. Names of cloned genes in this study are given after the accession numbers. Vertical bars on the right indicate corresponding order or order-family names.

Figure 2 Different phenotypic modifications in *BnCCR1-2ox* and *BnCCR2-4ox* plants.

(a) to (m) Plant phenotypes of different stages. Vegetative stage ([a] to [d]), middle-later bolting stage ([e] to [g]), flowering stage ([h] to [j]), harvest stage ([k] to [m]). Bending phenomenon of the upper stem of *BnCCR1-2ox* plants at late bolting stage (f) will disappear after flowering (i).

(n) and (o) root system at mature stage.

(p) and (q) Root system of one-week old seedlings, and the investigated values with statistic significance. Data represent means ± SD of at least 5 biological replicates. Asterisks indicate that means differed significantly from WT values (*P < 0.05; **P < 0.01, Student's *t* tests).

(r) Siliques at mature stage, indicating the wider siliques of *BnCCR1-2ox* and *BnCCRR2-4ox* compared with WT. Bar = 1cm.

Figure 3 Yellow seeds from T3 plants of *BnCCR1-2ox* and *BnCCR2-4ox* in contrast with black seeds from WT plants.

(a) and (b) seeds and seed coat cross-sections, highlighting the yellow-seed trait caused by seed color lightening by *CCR* overexpression. Bar = 50µm.

(c) extractable insoluble condensed tannins from seed coat, showing deeper color of *BnCCR2-4ox* as compared with *BnCCR1-2ox* and WT which implies easier extraction.

(d) 1000 seeds weight; (e) Seeds R value (higher value means deeper yellow color of the seeds coat); (f) Glucosinolates content (µmol/g); (g) Insoluble condensed tannins content of the seed coat. Data represent means ± SD of at least three biological replicates. Values are means ± SD of three biological replicates. Different letters behind the SD indicate statistically significant differences (one-way ANOVA, P < 0.05, Duncan's test).

Figure 4 *BnCCR1-2ox* and *BnCCR2-4ox* plants show differently fortified lignification patterns in various organs.

(a) to (c) Whole cross frozen stem-sections at early flowering stage ([a] and [b]), and whole cross free hand stem-section at harvesting stage (c). (a) Mäule staining; (b) and (c) phloroglucinol-HCl staining. Bar = 2mm.

(d) to (e) Cross-sections at mature stage of roots with more interfascicular fibers (d) and less interfascicular fibers (e), stained with phloroglucinol-HCl method. Bar = 500µm.

(f) to (j) Cross-sections of different parts of the stem at different developing stages. Middle-lower part of the stem at early flowering stage using Mäule

staining with different amplification folds ([f] and [g]). Middle-lower part of the stem at mature stage with phloroglucinol-HCl staining (h). Autofluorescence of the middle stem at early flowering stage under UV light with different amplification folds ([i] and [j]). if, interfascicular fiber; ph, phloem; pi, pith; xy, xylem. (f) and (i), bar = 200μm; (g), (h) and (j), bar = 80μm.

(k) to (n) Silique wall cross-sections at mature stage. Whole sections (k); Local sections ([l] to [n]). (k) to (l) Phloroglucinol-HCl staining; (M) and (N) Autofluorescence viewed under UV light. (k), bar = 500μm; (l) and (M), bar = 100μm; (N), bar = 50μm.

(o) to (q) Cross sections of the middle petiole with different methods. The whole cross-sections without any treatment (i); The vascular bundle with Mäule staining (p); The autofluorescence of the vascular bundle under UV light (q); bar = 50μm. (i), bar = 1000μm; (p), bar = 100μm; (q), bar = 50μm.

(r-t) Total lignin content analysis of stems (r), roots (s) and seed coats (t) was carried out by AcBr method. CWR, cell wall residue. Values are means ± SD of at least three biological replicates. Different letters above the bars indicate statistically significant differences (one-way ANOVA, $P < 0.05$, Duncan's test).

(u-x) Lignin monomer compositions of stems (u) and roots (v) were measured by thioacidolysis method. S/G ratios in stems and roots are displayed in (w) and (v), respectively. Values are means ± SD of at least three biological replicates. Different letters and values above the bars indicate statistically significant differences (one-way ANOVA, $P < 0.05$, Tukey's test) and respective percentage of the corresponding lignin monomers.

Figure 5 Secondary metabolites are distinctly modified in stems of *BnCCR1-2ox* and *BnCCR2-4ox* plants.

Secondary metabolites were determined by UPLC-HESI-MS/MS.

(a) Major soluble metabolites related to lignin pathway and its derivative pathways in the stems of ox1-5 and ox2-16 and WT, and see detail information in Table S5.

(b) Major soluble metabolites related to flavonoid pathway in the seeds of ox1-5 and ox2-16 and WT, and see detail information in Table S6. DP, degree of polymerization of the epicatechin unit.

(c) Major soluble metabolites related to glucosinolate pathway in the leaves of ox1-5 and ox2-16 and WT, and see detail information in Table S5.

Figure 6 Gene expression patterns of lignin, flavonoid and glucosinolate pathways are tremendously and differentially influenced in *BnCCR1-2ox* and *BnCCR2-4ox* plants.

(a) Transcript levels of the genes related to lignin biosynthesis in stems.

(b) Transcript levels of the genes related to flavonoid biosynthesis in seeds.

(c) Transcript levels of the genes related to glucosinolate biosynthesis in leaves. The *MYB29*, *CYP79F1* and *GSL* have no expression in WT, hence their expression level in *BnCCRox* is set relative to zero. The expression levels of other genes are set relative to WT. The yellow frame marks the genes involved in the synthesis of aliphatic glucosinolates. The red frame marks the genes involved in the synthesis of indole glucosinolates.

Figure 7 BnCCR1 and BnCCR2 play different roles in phenylpropanoid pathway.

The metabolic flux shifts in *BnCCR1-2ox* and *BnCCR2-4ox* plants are displayed in this map. The main route, which is conserved in angiosperms, is marked with the big background arrows (the general phenylpropanoid pathway is marked in light blue, while lignin-specific pathway is marked in brown). The blue arrows and names represent flux enhancement related to *BnCCR1-2ox*. Metabolites accumulation and related gene expression are increased in the stem of *BnCCR1-2ox*, indicating that overexpression of *BnCCR1* subfamily will significantly promote the biosynthesis of G- and H-lignin units. The purple arrows and names represent flux enhancement related to *BnCCR2-4ox*. Metabolites accumulation and related genes expression are increased in the stem of *BnCCR2-4ox*, indicating that overexpression of *BnCCR2* subfamily will

significantly promote the biosynthesis of S-lignin unit. The metabolites and the enzymes downregulated in both *BnCCR1-2ox* and *BnCCR2-4ox* plants are marked in green, whereas those with upregulation are in red. Unexpectedly, glucosinolates deposition and pathway gene expression are significantly and differently remodeled in *BnCCR1-2ox* and *BnCCR2-4ox* plants. Dashed arrows represent unknown or unauthenticated routes. Arrows with a question mark are suggested pathways in this study. Two successive arrows represent two or more metabolic conversions.

The enzymes and their abbreviations are as follows: ANR, anthocyanidin reductase; ANS, anthocyanidin synthase; CAD, cinnamyl alcohol dehydrogenase; 4CL, 4-coumarate:CoA ligase; C3H, *p*-coumarate 3-hydroxylase; C4H, cinnamate 4-hydroxylase; CCoAOMT, caffeoyl-CoA O-methyltransferase; CCR, cinnamoyl-CoA reductase; CHI, chalcone isomerase; CHS, chalcone synthase; COMT, caffeic acid *O*-methyltransferase; CSE, caffeoyl shikimate esterase; DFR, dihydroflavonol 4-reductase; F3H, flavanone 3-hydroxylase; F3'H, flavonoid 3'-hydroxylase; F5H, ferulate 5-hydroxylase; FLS, flavonol synthase; HCALDH, hydroxycinnamaldehyde dehydrogenase; HCT, hydroxycinnamoyl-CoA:shikimate/quinic hydroxycinnamoyl transferase; LAC, laccase; LDOX, leucoanthocyanidin dioxygenase; Med: mediator; PAL, phenylalanine ammonia-lyase; PER, peroxidase; SGT, sinapate 1-glucosyltransferase; SMT, sinapoylglucose:malate sinapoyltransferase; SST, sinapoylglucose:sinapoylglucose sinapoylglucosetransferase; UGT, uridine diphosphate glycosyltransferase.

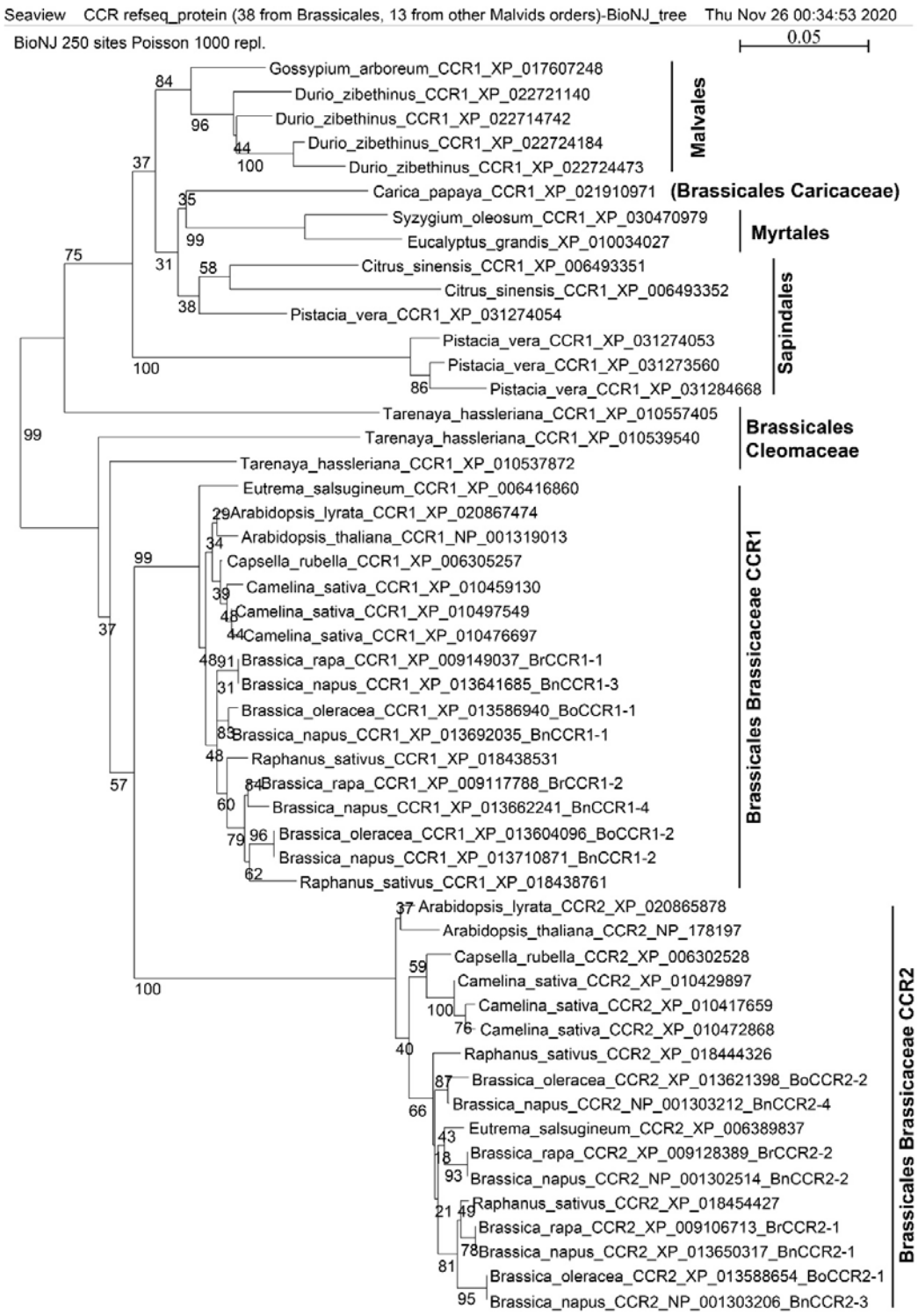
Seaview CCR refseq_protein (38 from Brassicales, 13 from other Malvids orders)-BioNJ_tree Thu Nov 26 00:34:53 2020
BioNJ 250 sites Poisson 1000 repl.
0.05
Gossypium_arboreum_CCR1_XP_017607248
Durio_zibethinus_CCR1_XP_022721140
Durio_zibethinus_CCR1_XP_022714742
Durio_zibethinus_CCR1_XP_022724184
Durio_zibethinus_CCR1_XP_022724473
Malvales
Carica_papaya_CCR1_XP_021910971
(Brassicales Caricaceae)
Syzygium_oleosum_CCR1_XP_030470979
Eucalyptus_grandis_XP_010034027
Myrtales
Citrus_sinensis_CCR1_XP_006493351
Citrus_sinensis_CCR1_XP_006493352
Pistacia_vera_CCR1_XP_031274054
Pistacia_vera_CCR1_XP_031274053
Pistacia_vera_CCR1_XP_031273560
Pistacia_vera_CCR1_XP_031284668
Sapindales
Tarenaya_hassleriana_CCR1_XP_010557405
Tarenaya_hassleriana_CCR1_XP_010539540
Tarenaya_hassleriana_CCR1_XP_010537872
Brassicales Cleomaceae
Eutrema_salsugineum_CCR1_XP_006416860
Arabidopsis_lyrata_CCR1_XP_020867474
Arabidopsis_thaliana_CCR1_NP_001319013
Capsella_rubella_CCR1_XP_006305257
Camelina_sativa_CCR1_XP_010459130
Camelina_sativa_CCR1_XP_010497549
Camelina_sativa_CCR1_XP_010476697
Brassica_rapa_CCR1_XP_009149037_BrCCR1-1
Brassica_napus_CCR1_XP_013641685_BnCCR1-3
Brassica_oleracea_CCR1_XP_013586940_BoCCR1-1
Brassica_napus_CCR1_XP_013692035_BnCCR1-1
Raphanus_sativus_CCR1_XP_018438531
Brassica_rapa_CCR1_XP_009117788_BrCCR1-2
Brassica_napus_CCR1_XP_013662241_BnCCR1-4
Brassica_oleracea_CCR1_XP_013604096_BoCCR1-2
Brassica_napus_CCR1_XP_013710871_BnCCR1-2
Raphanus_sativus_CCR1_XP_018438761
Brassicales Brassicaceae CCR1
Arabidopsis_lyrata_CCR2_XP_020865878
Arabidopsis_thaliana_CCR2_NP_178197
Capsella_rubella_CCR2_XP_006302528
Camelina_sativa_CCR2_XP_010429897
Camelina_sativa_CCR2_XP_010417659
Camelina_sativa_CCR2_XP_010472868
Raphanus_sativus_CCR2_XP_018444326
Brassica_oleracea_CCR2_XP_013621398_BoCCR2-2
Brassica_napus_CCR2_NP_001303212_BnCCR2-4
Eutrema_salsugineum_CCR2_XP_006389837
Brassica_rapa_CCR2_XP_009128389_BrCCR2-2
Brassica_napus_CCR2_NP_001302514_BnCCR2-2
Raphanus_sativus_CCR2_XP_018454427
Brassica_rapa_CCR2_XP_009106713_BrCCR2-1
Brassica_napus_CCR2_XP_013650317_BnCCR2-1
Brassica_oleracea_CCR2_XP_013588654_BoCCR2-1
Brassica_napus_CCR2_NP_001303206_BnCCR2-3
Brassicales Brassicaceae CCR2

Figure 1

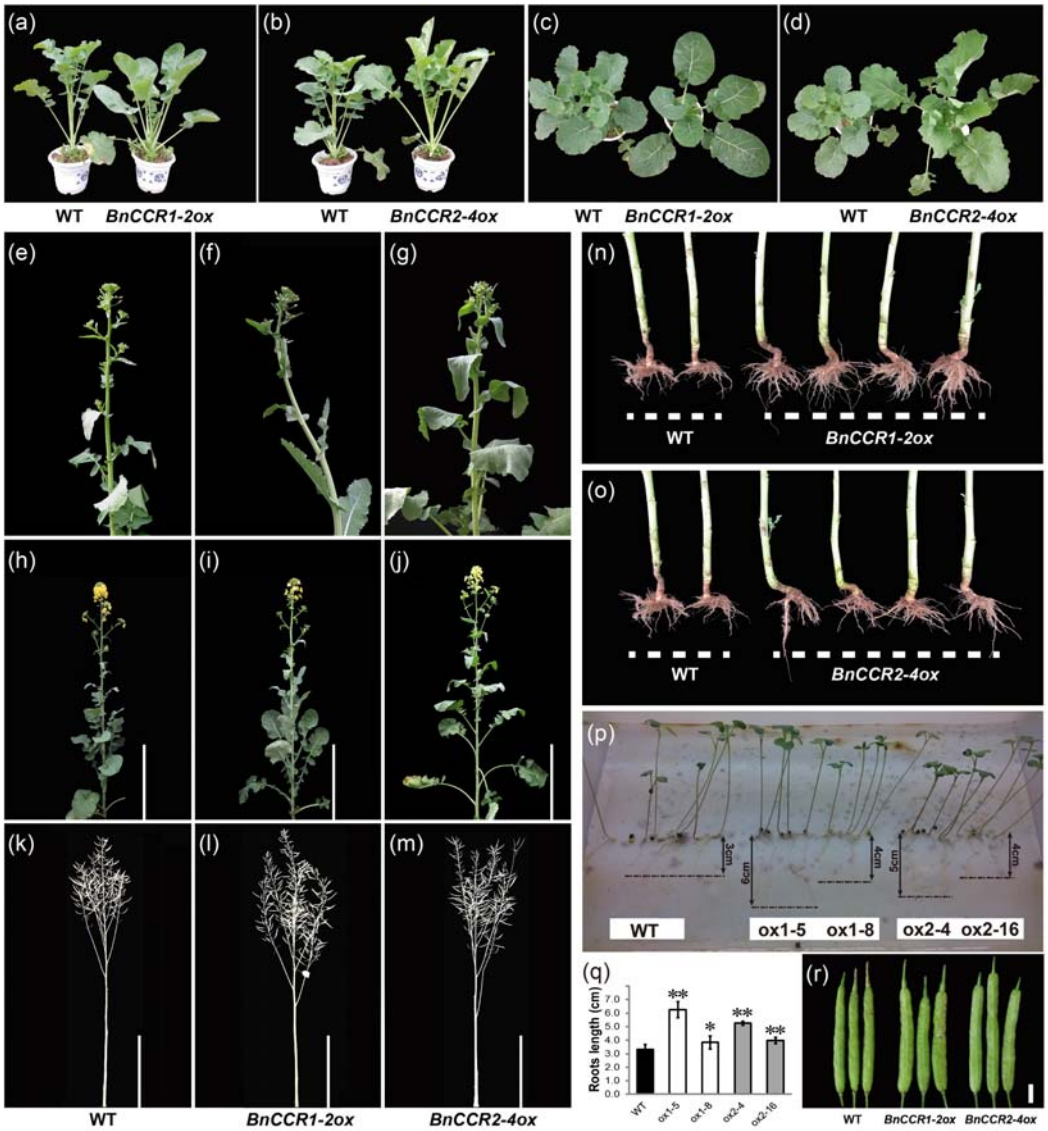
(a)
(b)
(c)
(d)
WT
BnCCR1-2ox
WT
BnCCR2-4ox
WT
BnCCR1-2ox
WT
BnCCR2-4ox
(e)
(f)
(g)
(n)
WT
BnCCR1-2ox
(o)
WT
BnCCR2-4ox
(h)
(i)
(j)
(p)
3cm
6cm
4cm
5cm
4cm
WT
ox1-5
ox1-8
ox2-4
ox2-16
(k)
(l)
(m)
(q)
Roots length (cm)
7.0
6.0
5.0
4.0
3.0
2.0
1.0
0.0
**
*
**
**
WT
ox1-5
ox1-8
ox2-4
ox2-16
(r)
WT
BnCCR1-2ox
BnCCR2-4ox
WT
BnCCR1-2ox
BnCCR2-4ox

Figure 2

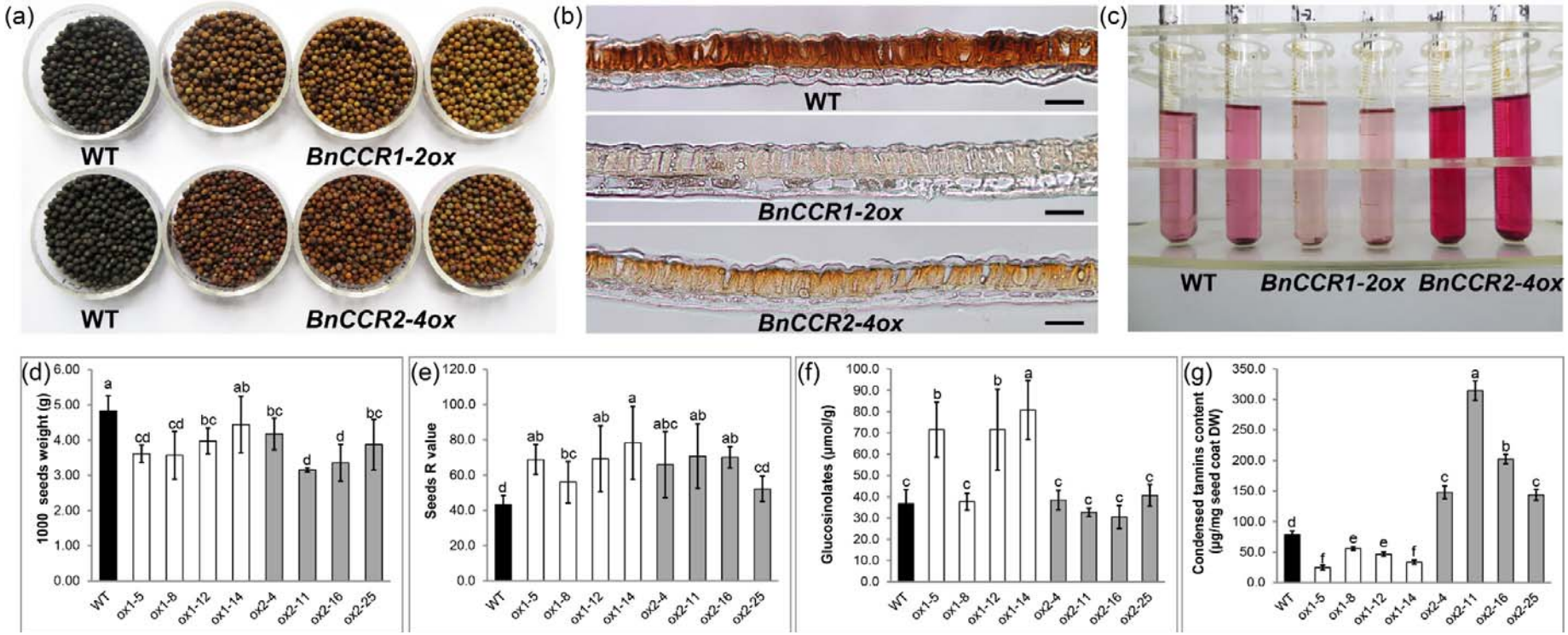
(a)
WT
BnCCR1-2ox
WT
BnCCR2-4ox
(b)
WT
BnCCR1-2ox
BnCCR2-4ox
(c)
WT
BnCCR1-2ox
BnCCR2-4ox
(d)
1000 seeds weight (g)
(e)
Seeds R value
(f)
Glucosinolates (μmol/g)
(g)
Condensed tannins content (μg/mg seed coat DW)
WT
ox1-5
ox1-8
ox1-12
ox1-14
ox2-4
ox2-11
ox2-16
ox2-25

Figure 3

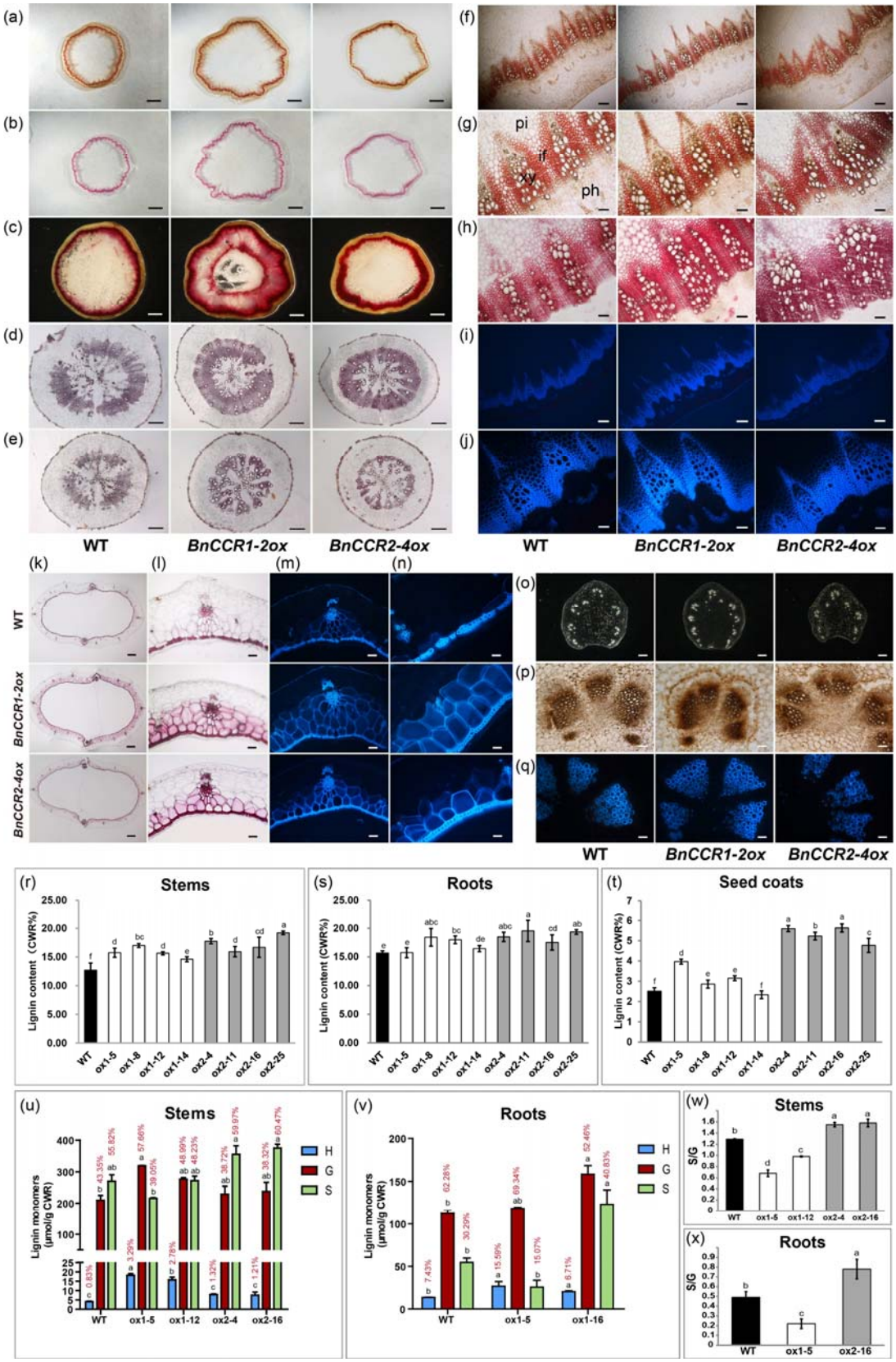
(a)
(b)
(c)
(d)
(e)
(f)
(g)
pi
if
xy
ph
(h)
(i)
(j)
WT
BnCCR1-2ox
BnCCR2-4ox
(k)
(l)
(m)
(n)
(o)
(p)
(q)
Stems
Roots
Seed coats
Lignin content (CWR%)
WT
ox1-5
ox1-8
ox1-12
ox1-14
ox2-4
ox2-11
ox2-16
ox2-25
(u)
(v)
(w)
(x)
Lignin monomers (μmol/g CWR)
H
G
S
S/G

Figure 4

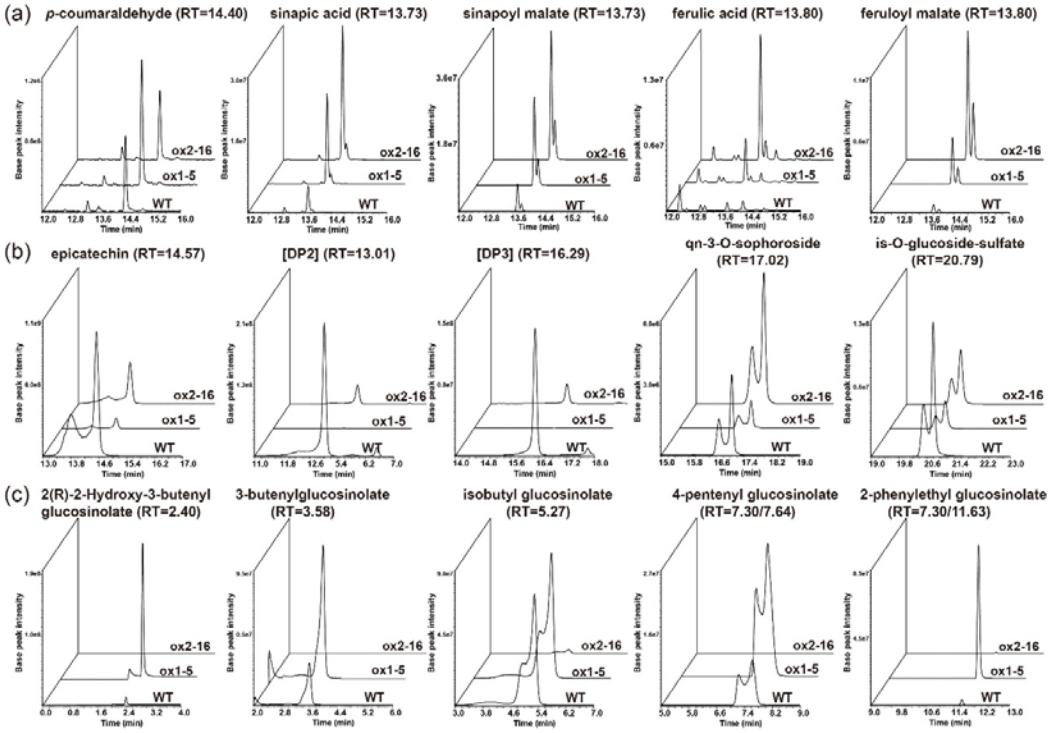
(a)
p-coumaraldehyde (RT=14.40)
sinapic acid (RT=13.73)
sinapoyl malate (RT=13.73)
ferulic acid (RT=13.80)
feruloyl malate (RT=13.80)
(b)
epicatechin (RT=14.57)
[DP2] (RT=13.01)
[DP3] (RT=16.29)
qn-3-O-sophoroside (RT=17.02)
is-O-glucoside-sulfate (RT=20.79)
(c)
2(R)-2-Hydroxy-3-butenyl glucosinolate (RT=2.40)
3-butenylglucosinolate (RT=3.58)
isobutyl glucosinolate (RT=5.27)
4-pentenyl glucosinolate (RT=7.30/7.64)
2-phenylethyl glucosinolate (RT=7.30/11.63)
ox2-16
ox1-5
WT
Time (min)

Figure 5

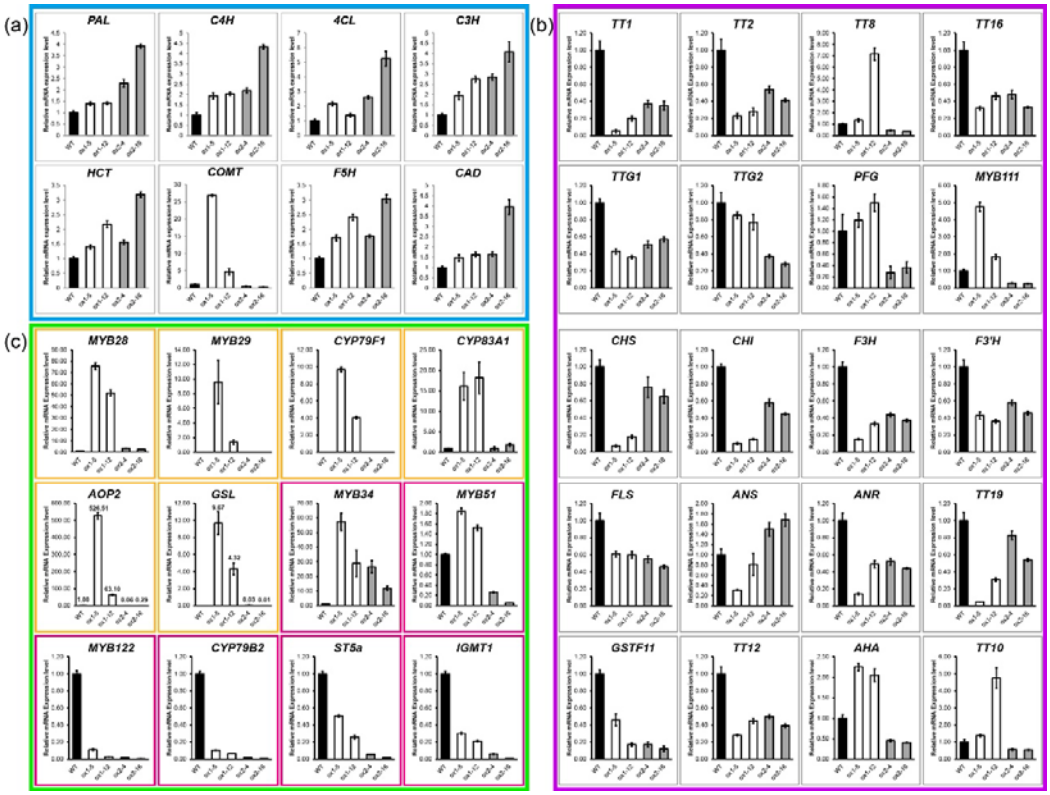
(a)
PAL
C4H
4CL
C3H
HCT
COMT
F5H
CAD
(b)
TT1
TT2
TT8
TT16
TTG1
TTG2
PFG
MYB111
CHS
CHI
F3H
F3'H
FLS
ANS
ANR
TT19
GSTF11
TT12
AHA
TT10
(c)
MYB28
MYB29
CYP79F1
CYP83A1
AOP2
GSL
MYB34
MYB51
MYB122
CYP79B2
ST5a
IGMT1

Figure 6

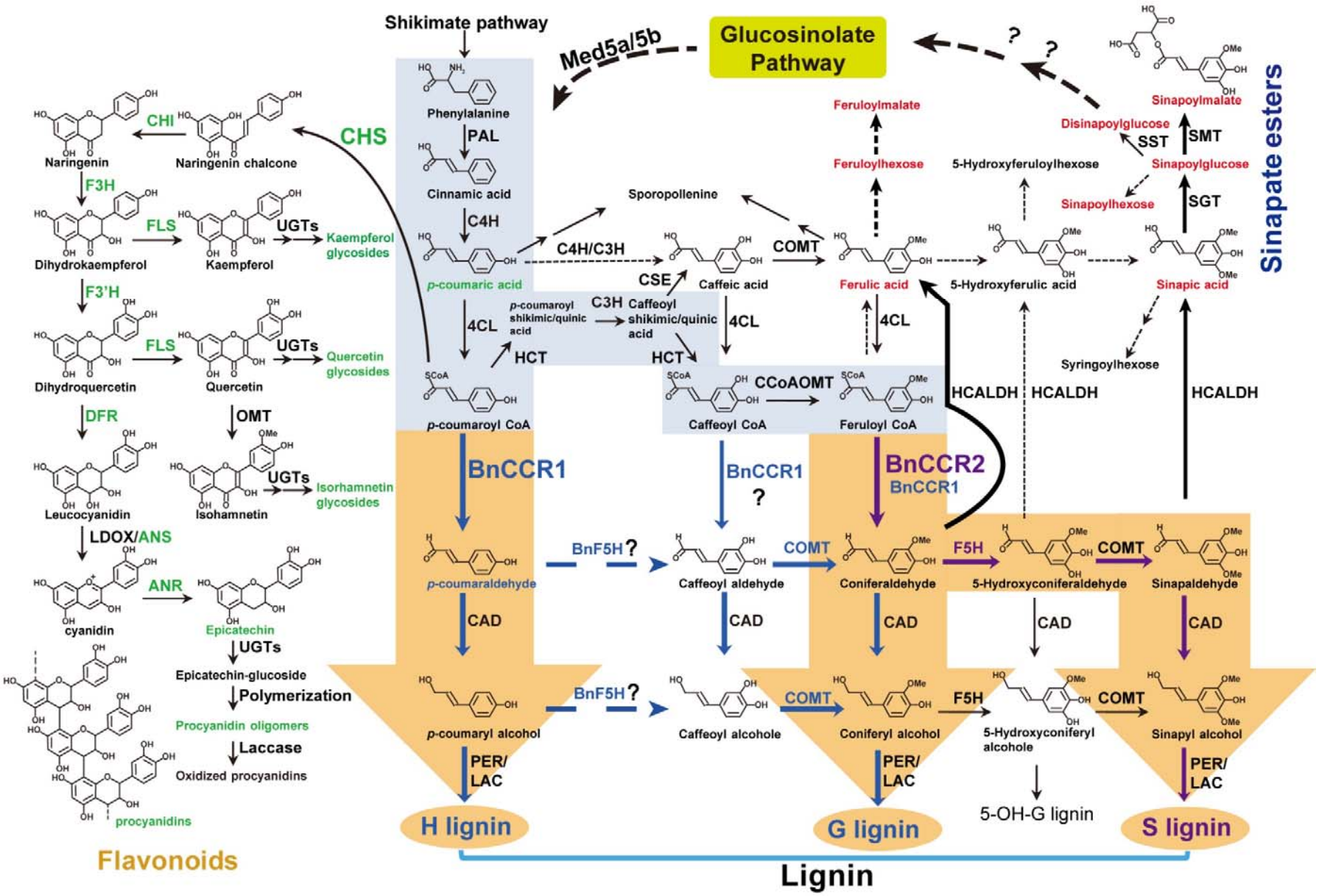
Shikimate pathway
Med5a/5b
Glucosinolate Pathway
Phenylalanine
PAL
Cinnamic acid
C4H
p-coumaric acid
4CL
p-coumaroyl CoA
HCT
p-coumaroyl shikimic/quinic acid
C3H
Caffeoyl shikimic/quinic acid
C4H/C3H
Sporopollenine
CSE
Caffeic acid
COMT
Ferulic acid
5-Hydroxyferulic acid
Sinapic acid
Feruloylmalate
Feruloylhexose
5-Hydroxyferuloylhexose
Sinapoylmalate
Disinapoylglucose
SST
SMT
Sinapoylglucose
Sinapoylhexose
SGT
Syringoylhexose
Sinapate esters
Caffeoyl CoA
CCoAOMT
Feruloyl CoA
HCALDH
BnCCR1
BnCCR2
BnF5H?
p-coumaraldehyde
Caffeoyl aldehyde
Coniferaldehyde
F5H
5-Hydroxyconiferaldehyde
Sinapaldehyde
CAD
p-coumaryl alcohol
Caffeoyl alcohole
Coniferyl alcohol
5-Hydroxyconiferyl alcohole
Sinapyl alcohol
PER/LAC
H lignin
G lignin
5-OH-G lignin
S lignin
Lignin
CHS
CHI
Naringenin
Naringenin chalcone
F3H
Dihydrokaempferol
FLS
Kaempferol
UGTs
Kaempferol glycosides
F3'H
Dihydroquercetin
Quercetin
Quercetin glycosides
DFR
OMT
Leucocyanidin
Isohamnetin
Isorhamnetin glycosides
LDOX/ANS
cyanidin
ANR
Epicatechin
Epicatechin-glucoside
Polymerization
Procyanidin oligomers
Laccase
Oxidized procyanidins
procyanidins
Flavonoids

Figure 7